Proceedings of the Sixth International Conference of NAEGE

VOLUME 5 **2022**

Printed in Nigeria by:
Cresolint Global Resources
+2348169836220 | cresolint@gmail.com

VOLUME 5 ISBN: 978-978-987-573-3 2022

PROCEEDINGS

of the

NAEGE

Sixth International Conference

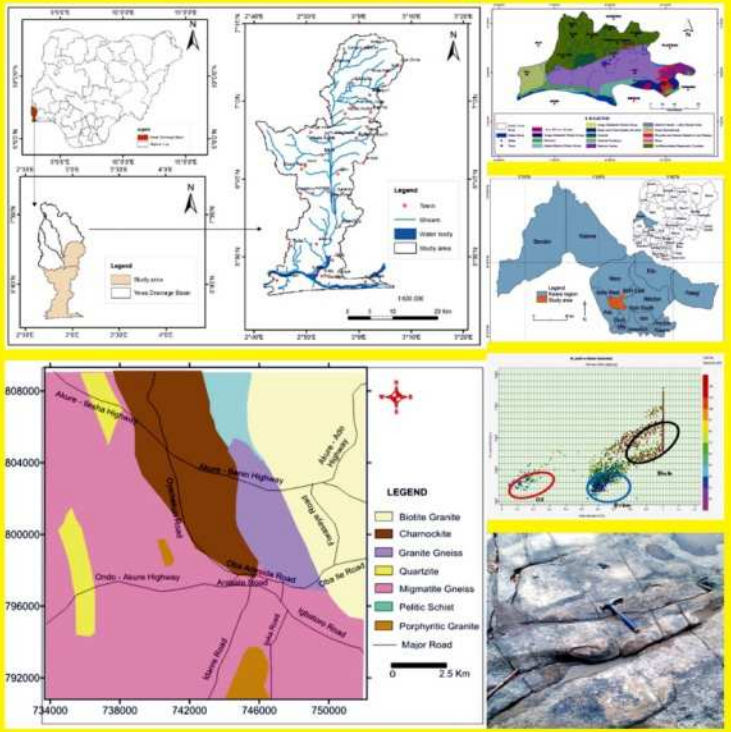

of the

NIGERIAN ASSOCIATION FOR ENGINEERING GEOLOGY AND THE ENVIRONMENT

Held at Ibadan, Nigeria

Proceedings

of the

SIXTH ANNUAL INTERNATIONAL CONFERENCE

"IBADAN 2021"

of the

Nigerian Association for Engineering Geology and the Environment

HELD BETWEEN 9TH AND 11TH SEPTEMBER, 2021
AT IBADAN, NIGERIA.

Publisher

Nigerian Association for Engineering Geology and the Environment

Editor-in-Chief
Dr. Ibrahim A. OYEDIRAN

Editorial Office
Department of Geology,
University of Ibadan,
Ibadan, Nigeria.
Tel: +234-8094718091
E-mail: oyediranibrahim2012@gmail.com

Subscription Rates
₦2,500.00 per copy (domestic)
US$100.00 per copy (foreign)

Printed in Nigeria by:

Suite 2, First Floor, Olowotinfowosanu Shopping Complex,
Iwo Road, Ibadan, Nigeria.
Tel: +234-816-983-6220; +234-805-394-1752
e-mail: cresolint@gmail.com, somoola04@yahoo.com

ISBN: 978-978-970-671-6

NIGERIAN ASSOCIATION FOR ENGINEERING GEOLOGY AND THE ENVIRONMENT

2022-2024 Executive Committee and Council Membership

President
Dr. Waliu K. ADEOLU, FNAEGE

Vice President (South)
Dr. Fidelis ABIJA, FNAEGE

Vice President (North)
Dr. (Mrs.) Salome WAZIRI, FNAEGE

General Secretary
Mr. Lukman A. AZEEZ

Assistant General Secretary
Dr. (Mrs.) Martina ANANABA

Editor-in-Chief
Dr. Ibrahim A. OYEDIRAN, FNAEGE

Deputy Editor-in-Chief
Dr. Ebiegberi OBORIE

National Treasurer
Dr. (Mrs.) Attah M. FAKEYE, FNAEGE

Financial Secretary
Dr. (Mrs.) Vivian OZOEKWE

Assistant Financial Secretary
Dr. Stephen E. OBRIKE

Publicity Secretary/PRO
Ms. Abimbola B. ALUKO, FNAEGE

Social Secretary/Special Duties
Mr. Frank E. IKUEWAN, FNAEGE

YEG Representative
Mr. Adebayo Olaniyi AFOLABI

IPP/Ex-Officio Member
Prof. Moshood N. TIJANI, FNAEGE

IAEG Vice President (Africa)
Prof. T.K.S. ABAM, FNAEGE

Patron
Prof. S.S. Malomo, FNAEGE

Fellows in Council
Prof. S.C. Teme, FNAEGE
Prof. Gabriel A. Adeyemi, FNAEGE

CONTENTS

ISBN: 978-978-970-671-6

Proceedings of the 6th International Conference of the Nigerian Association for Engineering Geology and the Environment (NAEGE), Ibadan, Nigeria, 7th - 11th September, 2021 (Vol. 5), 2022.

The Effect of the Landuse / Cover Changes on the Flood Patterns in Sub - Yewa Basin

Lamidi, R.B., Fakeye, A.M. and Okonufua, E.O.
Nigerian Building and Road Research Institute (NBRRI), Nigeria.
Corresponding E-mail: **bukkylam2003@yahoo.com**

Abstract
This study was carried out to assess the impact of landuse/cover changes on the flood patterns of sub- Yewa basin between the year 2002-2017. Landsat Satellite Imageries for the year 2002 and 2017 were analyzed to determine the extent and trend between the two periods while the Curve Number (CN) was calculated based on the US Soil Conservation System (SCS) model. The results showed that: The spatial extent of built-up area increased from 6.3% in 2002 to 12.7% in 2017, the forest decreased from 52.8% in 2002 to 33.7% in 2017 while the agricultural land increased from 25.8% in 2002 to 45% in 2017.The overall curve number was 75 in the 2002 image but increased to 79 in the 2017 image while the intensity of the peak flow has increased from 9.80m/s for 2002 to 12.91 m/s in 2017. The discharge rate of 2017 flood was greater than that of the 2002 flood, which is as result of the change in the stable forests to the unstable agricultural lands and urban settlement. The change in landuse/cover ought to be controlled in the weak districts and a few measures ought to be taken to adjustthe soil and vegetation cover**.**

Keywords*: Curve number, Peak flow, Landsat Imageries and Land use /cover*

Introduction

Land use change is a significant trademark in the runoff process that influences penetration, erosion, and evapotranspiration. Because of fast development, land cover is exposed to changes making many soils become impenetrable surfaces which lead to diminish in the soil penetration rate and subsequently increase the amount and rate of runoff. The significant changes in land use that influence hydrology are afforestation and deforestation, the escalation of farming, the waste of wetlands, road development, and urbanization (De Roo et al., 2001).

There are many evidences that change of land use have impacted the hydrological system of different river basins. These effects can be critical in small basins (Jones and Grant, 1996). The hydrological effects of land use change depend not just on the general changes in land use types, even so in their spatial distribution (Schumann and Schultz, 2000). However, it is more challenging to evaluate the effect of land use change on the precipitation runoff relations for enormous basin where the associations between land use, climatic qualities and the underlying hydrological processes are often mind boggling and dynamic (Uhlenbrook et al., 2001).

Khosrovshahi (2001) noted that the destructive floods have increased ten times in the past 50 years as result of continuous change in the natural cover of the land especially the forest lands, has decreased all over (Pouraghnyaii M.J, 2001.Likewise, Susswein et al. (2001) Bands et al., (1987) and Van Lill et al., (1980) explored the effect of forest cover on surface runoff and concluded that the change of land cover modifies the overland flow pattern**.**

Research in different fields have so far confirmed the ability and precision of remote sensing techniques in analyzing and mapping the land use patterns, which is a corner stone for all land use studies. Therefore, this study was carried out to assess the impactof land use changesonthe flood patterns between the of period of 2002-2017 using the GIS and remote sensing techniques. The specific objectives are to ascertain the land use types and how it has changed between 2002 – 2017; identify if these changes in land cover have had an impact on flooding; and, if so, then by how much

Method and Material

The Study Area

The Yewa drainage basin is a transboundary (international) river between the Republic of Benin and Nigeria.Yewa basin located in Southwestern Nigeria. The study area occupies a land area of 2118.4 km^2. The Yewa drainage basin is a transboundary (international) river between the Republic of Benin and Nigeria. The study area is situated within latitudes 6^0 15' 0"N and 7^0 45' 0"N of the equator and longitudes $2^0$42' 0"E and $3^0$0' 0"E of the Greenwich Meridian and has a total catchment area of about 4645 km^2as shown in Figure 1**.**

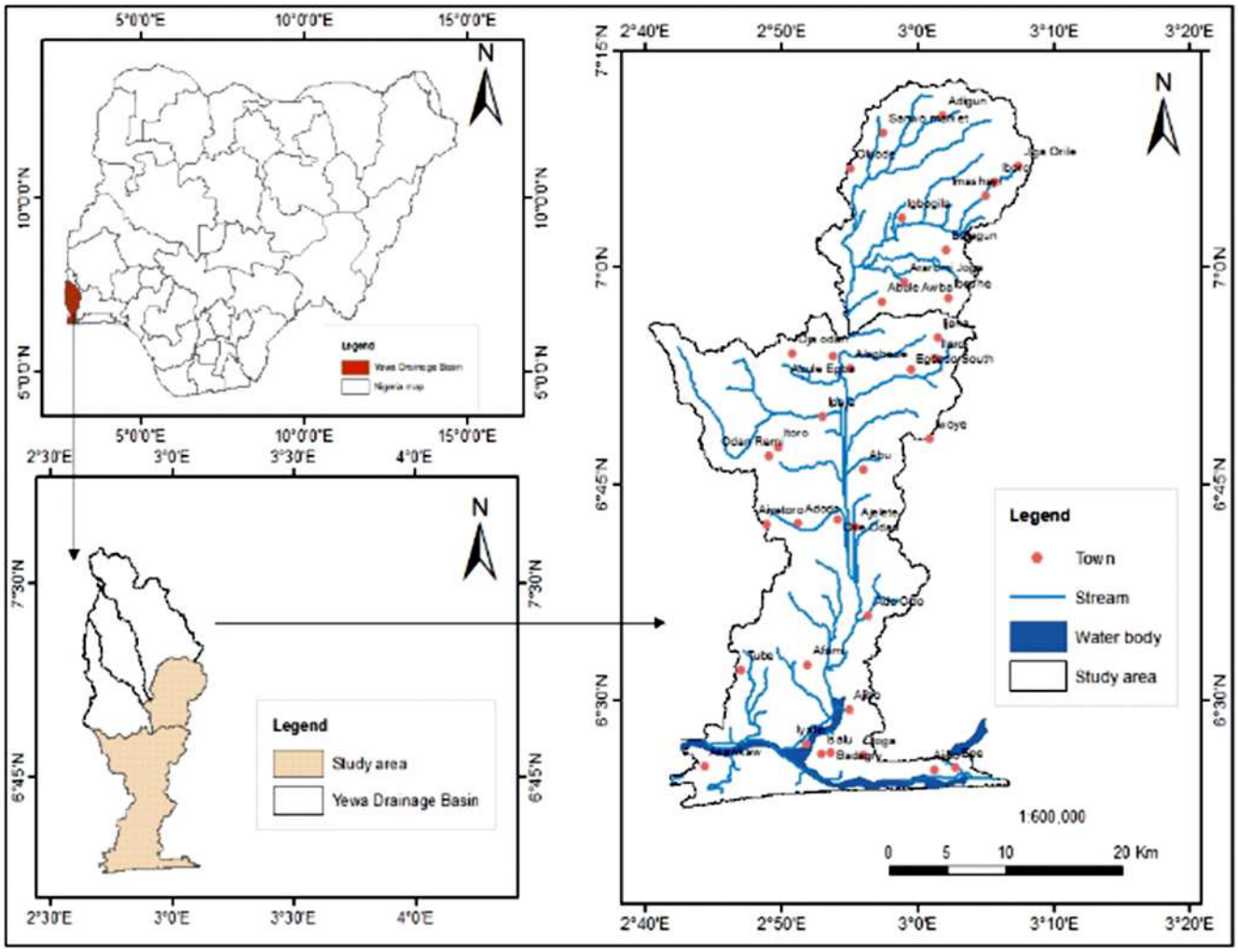

Fig. 1: The Study Area

Climate

In accordance to Koppen's climate classification, the Yewa River basin is located within the tropical rainy climate which is under the influence of the tropical continental (CT) and the tropical maritime (MT) air masses. The temperature varied from south to north in the basin, it has an average annual temperature of 26oC in the south and 28oC in the north with an annual range of ± 4o c. Rainfall in Yewa drainage basin also varied from south to north and it's generally decreases from the south to the north and varies from about 1500mm in the south to about 800mm in the north. Yewa basin is under the jurisdiction of the Ogun, Osun River Basin Development Authority which falls within Nigeria's hydrological Area 6. The projected annual population growth rate is about 2.77% and an annual runoff of 35.4*10 m or depth of runoff of 352mm per year (Federal Dept. of Water resources**,**1986**).**

Soil History

Soils in the study area are varied according to the geological history and soil formation processes in the different localities. The soils are derived from sedimentary rocks and are varied in their components and texture. Soils in the region are sandy and could only support savannah vegetation. The river valley has alluvial soils

Geology of the Study Area

The geology map for the study area was obtained from Nigerian Geological Survey Agency, 2003 – 2010 airborne survey index. The geology of the study area is basically sedimentary rock. The sedimentary rock of Yewa drainage basin consists of; Alluvial, Coastal plain sands (sands and clays), Ilaro formation (Sand clays and shale), Ewekoro formation (Shale and limestone),

Abeokuta formation (sands clays, calcareous parts) lying directly under the basement complex, Gneiss, migmatite complex and older granites series (Granitoids)

Data and sources

This investigation included both primary and secondary sources of data. The primary data includes visiting the study area to acquire the landuse reference point while the secondary include an administrative map of Nigeria, precipitation data, topographic data, soil data, and landuse data

Data Processing and Analysis

Digital elevation model (DEM) of 30m resolution from Shuttle Radar Topographic Mission (SRTM) was downloaded. The boundaries of the watershedwere extracted from the DEM using ARCSWAT extension in ArcGIS in which sub catchments 2, and 4 were chosen for this study and slope gradient was also generated from the DEM. The soil data collected were entered into excel creating a database which include percentage sand, clay and silt, soil types. The percentage sand, silt and clay were used to generate the hydrological soil group (HSG). The study area was visited to acquire the landuse reference data for image classification.

Land Cover Types and variation

Two series of Landsat images; 2002 and 2017 were downloaded. The maximum likelihood classifier was used to classify the image into different types of land cover (LC) which was to computethe extent of change and curve number.

Impact Assessment on flooding

To assess the impact of land cover changes on flooding, the proposed solution is based on estimating runoff volume and peak flow rate

Estimating Runoff factors

The runoff was estimated using the Soil Conservation Service (SCS) method developed by Mbajiorgu, 2004.

$$Q = \frac{(P-0.2S)^2}{(P+0.8S)} \quad \text{.....(1)}$$

Where Q = runoff volume; P = rainfall; S = retention parameter

The retention parameter is defined in terms of a curve number (CN) which depends on land use, and hydrologic soil condition (Mbajiorgu, 2004).
But:

$$S = \left(25400/_{CN}\right) - 254 \quad \text{.....(2)}$$

The curve number (CN) was computed by creating the boundaries of the basin, generating the hydrologic soil groups, Overlay the land use and hydrologic soil group maps to determine the area of each polygon and the CN for each unique polygon was calculate using the composite CN calculation

$$\mathbf{CNw}=\sum_{i=1}^{n} CNiAi/\mathbf{A_T} \quad \text{.....(3)}$$

Where Ai=is the area of different placesof study; $A_{T=}$ total area of interest.

According to infiltration rate, soils are classified into four HSG's (A, B, C, and D). The Hydrological Soil group was determined based on the percentages of clay, silt and sand content in the soil using the indicator for Hydrological Soil Group (HSG) as shown in Table 1.

Table 1: Indicator for Hydrological Soil Group (HSG)

S/N	HSG	Description
1	A	Soil with less than 10% clay and more than 90% sand
2	B	Soil with the clay content between 10-20% and 50% to 90% sand
3	C	Soil with the clay content between 20-40% and less than 50% sand
4	D	Soil with greater than 40% clay and less than 50% sand

Source: *NRCS, 2004*

Antecedent Moisture Condition presents the conditions of the area or watershed at the beginning of the storm. These conditions affect the amount of runoff generated from a particular storm event. The NRCS defined and used the following AMC condition

I. AMC I: low moisture dry
II. AMC II: average moisture
III. AMC III: high moisture due to heavy rainfall

In general CN are calculated for AMC II, then can be adjusted up to simulate AMC III or down to AMC I. AMC II was chosen and fair condition was chosen for treatment as recommended for area with lack adequate information.

The Peak flow Factor

The peak flow rate is the maximum runoff flow rate that occurs with a given rainfall event. The peak flow rate is

an indicator of the erosive power of a storm. In this study Peak flow rate is calculated based on Mbajiorgu, (2004) equation

qp= 0.0021QA Tp .....(4)
Where qp = peak flow rate in m/s; A = drainage area; Q = runoff in mm; TP = time of peak in hours.
Tp can be expressed as

tp = 1.1tc .....(5)
Where tc = time of concentration

According to Soil Conservation Service (SCS)Lag Equation (1973)

$$tc = 10L^{0.8}\left[\left(\frac{1000}{CN}\right) - 9\right]^{0.7} / (1900S^{0.5}) \quad \text{.....(6)}$$

Where t_c= time of concentration (min.); L = length of longest flow path (ft.); S = average slope.
CN = Soil Conservation Service (SCS) curve number.

To calculate the length of the longest flow path within a given basin which is often used to calculate the time of concentration of a basin. The hydrology analysis was carried out using ArcGIS Software of ESRI

Results and Discussion

The Land cover types and how it has changed between 2002 – 2017

Five classes of landcover were identified. The overall mechanical accuracy obtained was 80% and the kappa coefficient was 0.76. The result indicated that76% of image classification agreed with the reference data.The spatial extent of built-up area showed an increase, from 134km^2 (6.3%) in 2002 to 268.4 km^2 (12.7%) in 2017 of the total area. The forest area covered a total area of 1118km^2 (52.8%) in 2002 but decreased to 713.4km^2 (33.7%). Similarly, the area covered by water body decreased from 80km^2 (3.8%) in 2002 to 77.2km^2 (3.6%) in 2017; the areas covered with bare ground decreased from 239.4km^2 (9.3%) to 106.4 km^2 (5%) in 2017 while the agricultural land was increased from 547km^2 (25.8%) in 2002 to 953km^2 (45%) in 2017 (figure 2 and 3) at the expense of the natural lands such as vegetation and bare lands, the increase in agricultural lands and builtup area is as a result of population growth of the Basin.

The Runoff Parameters

The runoff parameterscomputed includes; retention parameter, Curve number, rainfall data, hydrological soil group (HSG)

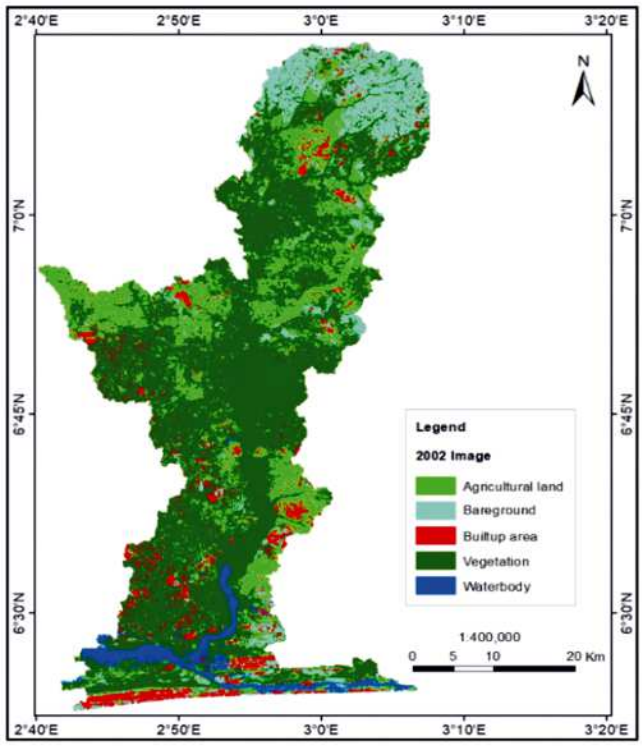

Fig. 2: Landcover classes (2002)

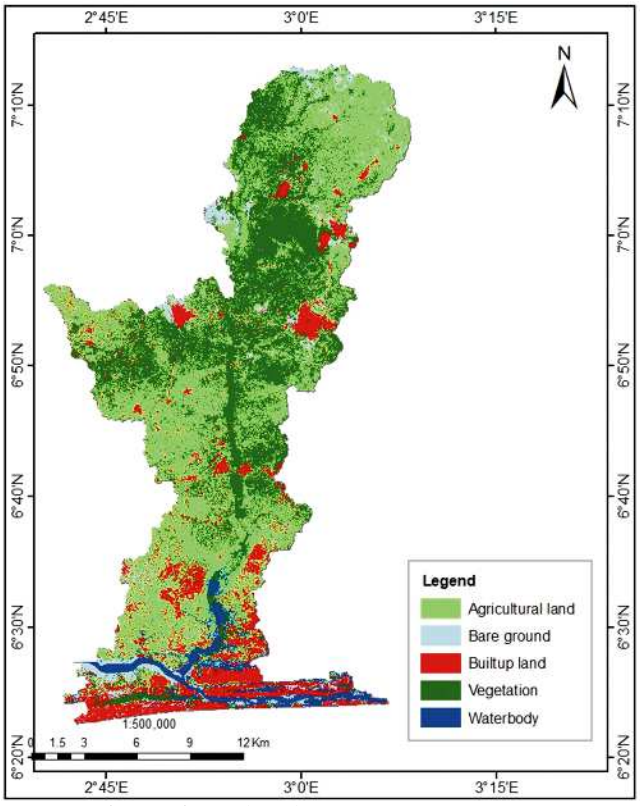

Fig 3: Landcover classes (2017)

Hydrological Soil Group (HSG)

The hydrological soil group computed reveals that the soil types in the study area fell into four hydrological soil groups (A, B, C, and D) as shown Table 1. The group A soil covered a total area of 612.4km^2 (28.9%) and it signifies soils having a low runoff potential due to high infiltration rates, group B soil covered the total area of 622km^2 (29.4%) which signifies soils having a moderately low runoff potential due to moderate infiltration rates, group C covered 761km^2 (35.9%) of the study area that indicates soils with moderately high runoff potential due to slow infiltration rates while the group D soil covered 123km^2 (5.8%) of the total area, is the soils having a high runoff potential due to very slow infiltration rates as shown in Figure 4 and Table 2.

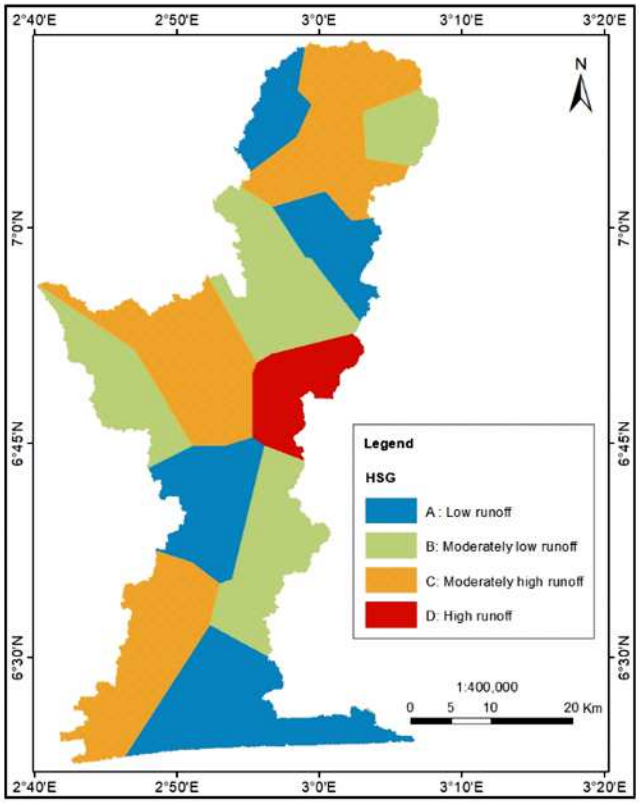

Fig. 4: Hydrological Soil group map

Table 2: Spatial distribution of Hydrological soil group

S/N	HSG	Area km^2	Area%
1	A	612.4	28.9
2	B	622	29.4
3	C	761	35.9
4	D	123	5.8
		2118.4	100

Curve number computation

Table 3 and 4 show the result for computed curve number for 2002 and 2017 respectively.

Table 3: Composite Curve number for 2002.

S/N	Landcover	Area km^2	A	B	C	D	CN*Area/Total Area
1	Agricultural land	547	72	81	88	91	45401
2	Builtup land	134	49	69	79	84	9413.5
3	Forest	1118	45	66	77	83	75744.5
4	Bare ground	239.4	77	86	91	94	20827.8
5	Waterbody	80	100	100	100	0	8000
		3305.8					159386.8/2118.4

CN_w= 159386.8/2118.4 = 75.25 = CN_w=75 for 2002

Table 4: Composite Curve number for 2017

S/N	Landcover	Area km^2	A	B	C	D	CN*Area/Total Area
1	Agricultural land	953	72	81	88	91	79099
2	Builtup land	268.4	49	69	79	84	23350.8
3	Forest	713.4	45	66	77	83	48332.85
4	Bare ground	106.4	77	86	91	94	9256.8
5	Waterbody	77.2	100	100	100	0	7720
		3305.8					167759.45/2118.4

CN_w= 167759.45/2118.4 = 79.19 = CN_w=79 for 2017

Estimation of Runoff Volume

The computed value for surface storage were 85mm (3.35Inches) in 2002 and 68mm 9(2.68Inches) in 2017 while the initial abstraction was computed to be 17mm (0.63Inches),13.5mm (0.55Inches) respectively. The runoff computed was 43.9mm (1.73In or 0.14ft) in 2002 and 51.4mm (2.02In or 0.17ft), the total drainage area is 2118.4km^2 (523468.04acres or 22802267826.758ft)as shown in Table 5.

Table 5: Runoff and peak flow analysis

S/N	Storm Date	Rainfall (mm)	Rainfall (In)	Q (mm)	Q (In)	Peak flow rate (m/s)
1	18-10-2003	103.8	4.09	43.9	1.73	9.80
2	1911-2017	103.8	4.09	51.4	2.02	12.91

Estimation of Peak Flow Factor

The drainage area is 2118.4km^2 (523468.04acres or 22802267826.8ft), the runoff value is 43.9mm (1.73In or 0.14ft) for 2002 and 51.4mm (2.02In or 0.17ft) for 2017 respectively. The computed value for the length of longest flow path was 273707.7ft (Figure 5), the CN value are 75 and 79. The average slope for the basin is 3.5%. The computed value for tc is 176 and 156 while TP values are 194 and 172. The peak flow computed was 9.80m/s in 2002 and 12.91m/s in 2017 respectively .

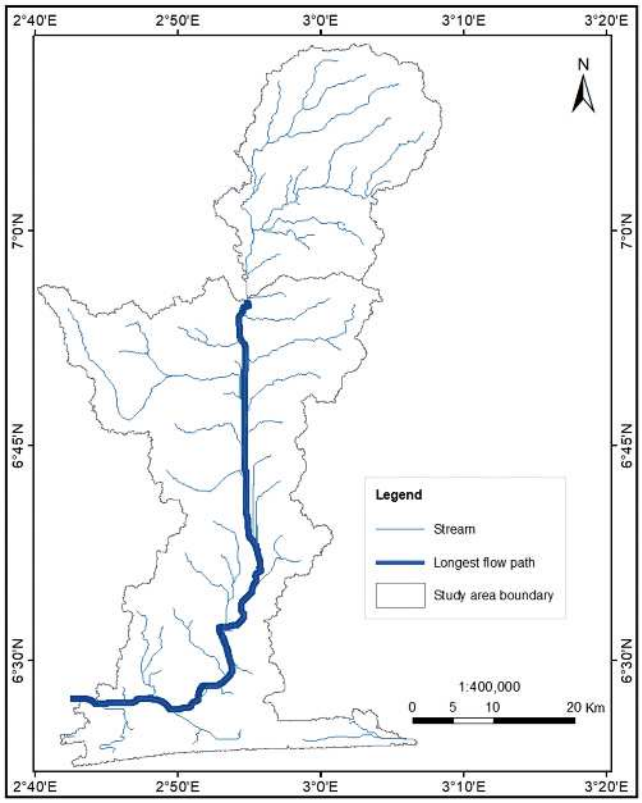

Fig. 5: Longest flow path location

Discussion

Based on the image classification, there seems to be remarkable negative change from 2002 to 2017 in vegetation and bare lands. Bare landsdecreased with about 6.3% and vegetation lands decreased by 19.1% in 2002 but in 2017 agricultural land increased by 19.2% while built-up area increased by 6.4%. Because of these cycles, the Curve Number has expanded by 4% while the surface water retention capacity decreased from 17 to 13.6. Likewise, the runoff rate has expanded from 43.9 to 51.4. The peak discharge has expanded from 9.80m/s in 2002 and 12.91m/s in 2017 respectively. The land cover change and the Curve Number increase are indications of more flooding in the Basin. The runoff and peak discharges of the Basin also increased during the 2017 flood. Vegetation lands are one of the components of the steady state in which every component depended on for complete and ideal capacity. But when these natural sources were destroyed and changed to the agricultural lands and urban development, it will affect their texture, drainage and even water retention capacity.

Conclusion

The comparison of the land use/cover types of the two images of 2002 and 2017, indicated that the area of the bareland, vegetation areas, have decreased about 6.3 and 19.1% respectively. But the agricultural land and builtup area have increased about 19.2 and 6.4% respectively. It seems that most of the land cover change has happened into the agricultural lands due to the inflow of population into Basin. On the other hand, the higher rate of farming and urban development has put much pressure on the lands and has decreased their fertility. These variables have expanded the flood limit and overflow force of the Basin. The lessening of vegetation force because of the cultivating has likewise expanded the runoff limit of the Basin. Because of these cycles, the Curve Number has expanded about 4% during the examination time frame. Likewise, the runoff rate has expanded from 43.9 to 51.4. That is, 2017 values have expanded more than the 2002 values. In this way, the continuation of the land cover change is turning into a genuine danger to the Basin. This ought to be considered by the advancement organizers of the Basin. The land cover change ought to be controlled in the weak districts and a few measures ought to be taken for the adjustment of the soil and vegetation cover. The comparison of the two hydrographs and the adjustment of the land cover types featured this point that the land cover is considerably more essential to the normal asset's.

During these floods, in spite of the equivalent measure of rainfall, the 2017 flood delivered higher run off than the 2002 flood. The solitary justification which is the destruction of the natural resources and their transfer to the unstable farm lands and urban development. It is highly suggested that the natural resources managers and planners should think about this finding and put into consideration and prevent the increasing destruction of the land sources. Else, we ought to expect the heavy floods like the one of August 2012 to an ever-increasing extent.

References

J. K. Lorup, J. C. Refsgaard and D. Mazimavi, "Assessing the Effect of Land Use Change on Catchment Runoff by Combined Use of Statistical Test and Hydrological Modeling. Case Studies from-Zimbabwe," Journal of Hydrology, Vol. 205, 1998, pp. 147-163.

A. Loukas, L. Vasiliades, and N. R. Dalezios, "Flood Producing Mechanisms Identification in Southern British Clombia, Canada," Journal of Hydrology, Vol. 277, 2000, pp. 218-235.

Solaimani, K. Modallaldoust, S. and Lotfi, S. (2009): Investigation of Land Use Changes on Soil Erosion Process Using Geographical Information System. Int. J. Environ. Sci. Tech., 6, (3): 415 424

Wahren, A., Feger, K.H., Schwarzel, K. and Munch, A. (2009): Land-Use Effects on Flood Generation – Considering Soil Hydraulic Measurements in Modelling. Adv. Geosci., 21: 99–107.

De Roo, A., Odijk, M., Schmuck, G., Koster, E. and Lucieer, A. (2001): Assessing the Effects of Land Use Changes on Floods in the Meuse and Oder Catchment. Physics and Chemistry of the Earth, Part B: Hydrology, Oceans and Atmosphere, 26: 593–599

Jones, J. A. and Grant, G. E. (1996): Peak Flow Responses to Clear-Cutting and Roads in Small and Large Basins, western Cascades, Oregon. Water Resour. Res. 32, (4): 959-974.

Schumm, A. H. and Schultz, G. A. (2000): Detection of Land Cover Change Tendencies and Their Effect on Water Management. Remote Sensing in Hydrology and Water Management, Chapter 19, Springer-Verlag

Uhlenbrook, S., Mc Donnell, J. and Leibundgut, C. (2001): Foreword to the Special Issue: Runoff Generation and Implications for River Basin Modelling, Freiburger Schriften zur Hydrologie, 13: 4–13

Bands, D. P., Bosch, J. M., Lamb, A. J., Richardson, D. M., Van Wilgen, B. W., Van W. and Versfeld, D.B. (1987): Jonkershoek Forestry Research Centre Pamphlet 384, Department of Environment Affairs, Private Bag X447 Pretoria.

Susswein, P. M., Noordwijk M. and Verbist, B.(2001): Forest Watershed Functions and Tropical Land Use Change. International Centre for Research in Agroforestry. Southeast Asian Regional Research Programme

Van Lill, W. S., Kruger, F. J. and Van Wyk, D. B. (1980): The Effects of Afforestation with Eucalyptus Grandis (Hill Ex Maiden) And Pinus Patula (Schlecht. Et Cham.) on Streamflow from Experimental Catchments at Mokobulaan, Transvaal. J. Hydrol., 48: 107–118

M. Khosrovshahi, "Determining the Role Sub-Basins in the Flood Intensity of Damavand Watershed," Master's Thesis, University of Tarbiat Modarres, Tehran, Iran, 2001.

ESRI (2006) Arc GIS Software of ESRI

M. J. Pouraghnyaii, "The Effect of Vegetation Changes in the Flood Regime of Neka River Watershed Basin," Master's Thesis, University of Tehran, Tehran, 2001.

M. N. Shrestha, "Integrated ANN Modeling for Assessment of Runoff Due to Land-use Change Using Remote Sensing and GIS," 2000. http://www.gisdevelopment.net

NRCS. 2004. National Engineering Handbook. Part 630 Hydrology, 210-VI-NEH-630.10. US Department of Agriculture, Washington DC

Mbajiorgu, C.C. (2004). Determination of Watershed BMPs for Soil and Water Conservation Using AGNPS. Journal of Agricultural Engineering and Technology, (12): 115 – 142

ISBN: 978-978-970-671-6

Proceedings of the 6th International Conference of the Nigerian Association for Engineering Geology and the Environment (NAEGE), Ibadan, Nigeria, 7th - 11th September, 2021 (Vol. 5), 2022.

Investigation of Geotechnical Properties of Lateritic Soil Stabilized with Cassava Peel Ash for Use in Road Construction

Ologun, S., Aboluwarin, O.M., Arigi, A.D. and Akinyeye, O.J.

Nigerian Building and Road Research Institute, KM 10 Idiroko Road Ota, Ogun State, Nigeria.

Corresponding E-mail: **sehindeologun@yahoo.com**

Abstract

Road pavement failure is a major problem in Nigeria which could be due to a number of factors. Several researchers had used cement, lime, bitumen and lean concrete to improve properties of weak soils which constitutes to high cost of construction owing to their expensive nature. This research work is to determine the effect of cassava peel ash on geotechnical properties of lateritic soil as stabilizing agent for sub-grade soil in road construction. The lateritic material (sub-grade) used was obtained from a highway construction work at a Federal road in Akure, Ondo State. The soil sample was collectedat a depth of 0.7m and sealed in a sack. Cassava Peel Ash (CPA), that was used as a stabilizing agent was obtained from Ogbese, in Akure North Local Government Area of Ondo State, Southwestern Nigeria. The sample were subjected to tests such as Natural moisture content, Sieve analysis, Compaction, California Bearing Ratio (CBR), and Unconfined Compression Strength Test(UCS) to determining their geotechnical properties after adding 0, 4, 8, 10 and 12% Cassava Peels Ash (CPA) by weight of sample to the soils. The CBR values obtained from the results of lateritic soil was 32% while the optimum CBR value obtained for the stabilized lateritic soil was 46% at 8% CPA content. The UCS values at 0, 4, 8, 10, and 12% were 120.70, 575.50, and 500, 150 and 475kN/m^2 respectively. The effect of CPA stabilization on the geotechnical properties of lateritic soil brings considerable improvement on the physical and engineering characteristics of the lateritic soils as evident in the results. Therefore at 8% Cassava Peels Ash (CPA) has the potential to effectively stabilize lateritic soils and can be used as a sub-grade and sub base materials in road construction.

Keywords*: Cassava Peel Ash (CPA), Stabilization, Lateritic Soil, California Bearing Ratio (CBR.) and Compaction*

Introduction

Soil Stabilization is being used for a variety of engineering works, the most common application is in the construction of roads and highway pavements, where the main objective is to increase the strength or stability of the underlying soil and to reduce construction cost by making the best use of locally available materials. Soil improvement could either be by modification or stabilization, or both. Soil modification is the addition of a modifier (cement, lime, etc.) to a soil to change its index properties, while soil stabilization deals with the treatment of soils to enable their strength and durability to be improved such that they become totally suitable for construction beyond their original classification (Alhassan,2008). Soil stabilization is the process of improving the shear strength parameters of soil and thus increasing the bearing capacity of soil. It is required when the soil that is available for construction is not suitable to carry structural load. Soil Stabilization can also be described as the alteration of soils to enhance their physical properties. It can also lead to increase in the shear strength of a soil or control the shrink-swell properties of a soil, thus improving the load bearing capacity of a sub-grade to support pavements and foundations. Soil stabilization is used to reduce permeability and compressibility of the soil mass in earth structures and to increase its shear strength (Amuu, *et al*, 2004).The common soils that are majorly used are lateritic soils and are majorly used in the country. It has been generally discovered by researchers that some laterite have low bearing capacity and low strength due to high content of clay. When lateritic soil contains a large amount of clay materials its strength and stability cannot be guaranteed under load especially in the presence of moisture (Alhassan, 2008).

The soil whose parent rock came out through weathering have been widely known by several people as a residual of rock decay that is red, reddish brown and yellowish in color and which have a high content of oxides of iron and hydroxides of aluminum and low proportion of silica (Bello and Adegoke, 2013).

Lateritic soils have been made to blend with several chemical additives to make it useful for construction. This has to deal with changing the engineering property of laterite (Amuu and A detuberu,2010).

For several years, several materials have been used for stabilizing soils in which cement and lime have been the two main materials. These materials have rapidly increased in price due to the sharp increase in the cost of energy and high demand for them. It has been shown by (Bello *et al.*, 2014) that Portland cement, by the nature

of its chemistry, produces large quantities of carbon dioxide (CO_2) for every ton of its final product which contributes to the melting of the ozone layer covering the earth surface. Therefore, replacing proportions of the Portland cement in soil stabilization with agricultural waste material like Cassava Peels Ash (CPA) will reduce the overall environmental impact of the stabilization process.

CPA is cassava peel that has been dried and burnt into ashes. Cassava peel constitutes between 20-35% of the weight of tuber, especially in the case of hand peeling. Based on 20% estimate, about 6.8 million tons of cassava peel is generated annually and 12 million tons are expected to be produced in the year 2020 (Amuu and Adetuberu,2010).Waste like cassava peels should have been dispose normally on a dumpsite or given to animals that can easily feed on them. At the same time, the major challenge in our environment is the indiscriminate disposal of cassava peels due to one reason or the other which include lack of utilization of wastes which include cassava peels. Therefore, the aim of this study is to investigate the effect of CPA on the stabilization of lateritic soils. The main objective of the research work is the effect of stabilization on weak soil sample with (CPA) to increase the strength and bearing capacity of the soil.

Location and Geology of the Study Area

The study area lies within Latitudes 07^0 09' and 07^0 19'N and Longitudes 05^0 07' and 05^0 17'E. The metropolis is located on a gently undulating terrain surrounded by isolated hills and inselbergs. Topographic elevations vary between 260 and 470 m above sea level (Owoyemi, 1996). The area around the Akure Metropolis is underlain by the Basement Complex rocks of Southwestern Nigeria. The petrological units include Migmatite-Gneiss-Quartzite Complex, Charnockitic and Dioritic rocks, Older Granites and Unmetamorphosed dolerite dykes (Rahaman,1988).

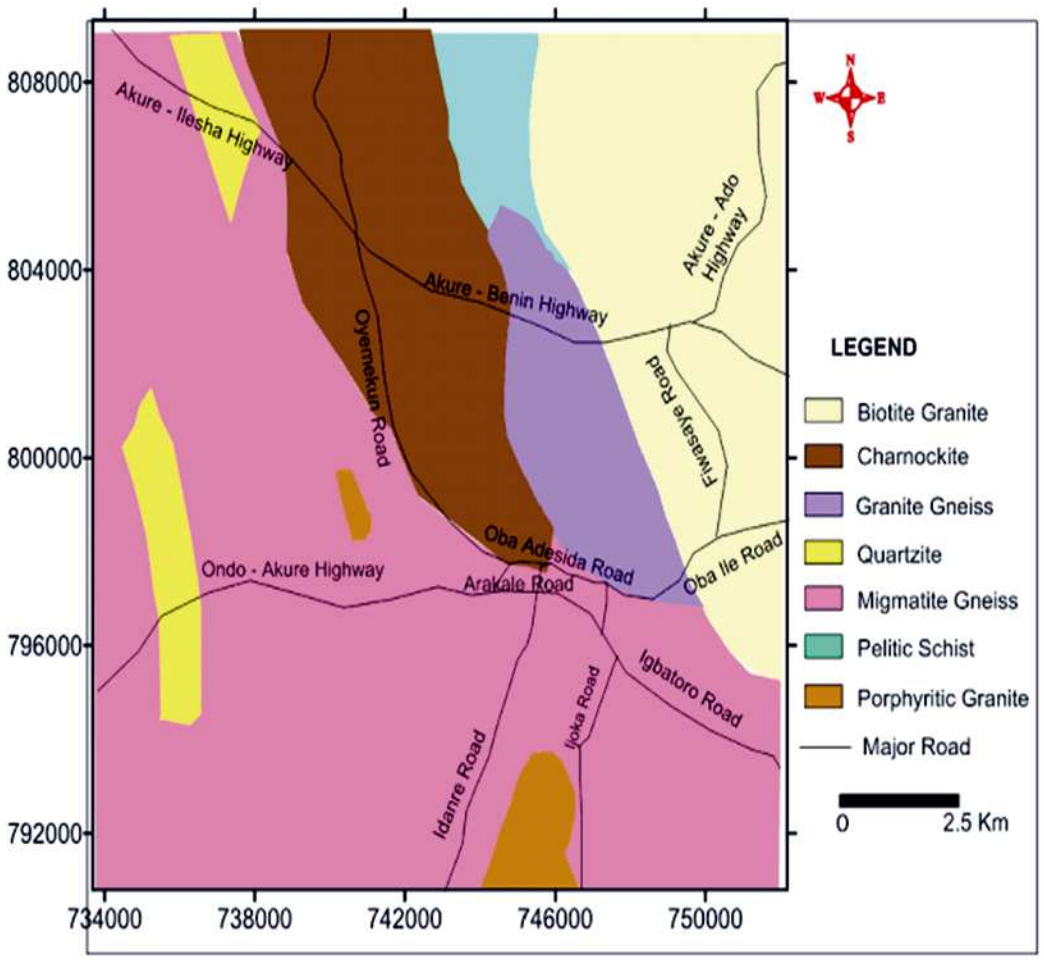

Fig. 1: Geological Map of Akure Metropolis (After Owoyemi, 1996)

Materials and Method

The lateritic soil material used was obtained from a borrow pit in Akure, Ondo State. The soil sample was taken at a depth of 0.7m and sealed in a sack. The soil sample was air dried to obtain particles passing through the 275mm sieve. CPA that was used as a stabilizing agent for this research was obtained from Ogbese, Akure North Local Government Area of Ondo State, Southwestern Nigeria. A partially dried sample of CPA was obtained from the source. It was gathered together and sun-dried before burning into ash using an open incinerator for about 650^{0}C. The ash was allowed to cool, gathered and well ground. After grinding, it was passed through a 0.075 mm sieve. CPA was subjected to X-ray Fluorescence (XRF) test to determine its oxide compositions. The lateritic sub-grade soil was stabilized by mass of soil in the following percentage replacements: 0, 4, 8, 10 and 12%.The blends were subsequently subjected to Natural Moisture Content, Sieve Analysis, Specific Gravity, Atterberg Limit, Compaction Test, CBR (unsoarked)and UCS according BS 1377 (1990).

Result and Discussion

Chemical (Oxides) Composition OF CPA

From Table 1, CPA contains 59.72% SiO_2, 11.10% Al_2O_3 and 1.52% Fe_2O_3. This aggregation of these oxides gives 72.34% which is in line with ASTM C 618-78 requirement of 70% minimum for pozzolanas. Thus, CPA meets the requirement for a pozzolana. The LOI of 5.07% and SO_3 of 2.08% all fall within agreeable limits. CPA was classified as class F pozzolana after fulfilling all above highlighted criteria.

Table 1: Results of Chemical Composition of CPA

Parameter	Units(%) Chemical composition
SiO_2	59.72
Al_2O_3	11.1
Fe_2O_3	1.52
CaO	8.42
MgO	5.22
SO_3	2.08
K_2O	6.82
Na_2O	0.05
LOI	5.07

Natural Moisture Content

This describes the amount of moisture present at the time of sub-grade sample collection and storing in the laboratory. The natural moisture content obtained was average of 24.7%.

Specific Gravity Test

The value of the specific gravity for the natural soil sample was 2.25

Index Properties of Soil

The index properties of the natural soil are summarized in Table 2. The percentages passing the No. 200 sieve was 37.60% as indicated in Figure 2. The atterberg limits results showed that the Liquid Limit (LL), Plastic Limit (PL) and Plasticity Index (PI) of the lateritic sub-grade soil were 42.20, 23.50 and 18.70% respectively. The PI falls in the range of 10 – 25% which according to (Mitchell 1976) indicate that the soil is of medium plasticity. The soil sample was classified as A-6 according to the AASHTO soil classification system (AASHTO, 1986).

Table 2: Properties of the Soil Sample

Natural moisture content	24.7
Liquid limit(%)	42.20
Plastic limit(%)	23.50
Plasticity Index (%)	18.70
Specific gravity	2.25
Percentage passing No. 200 Sieve (%)	37.60
AASHTO Classification	A - 6
MDD[kg/m^3]	1.75
CBR [%]	32
UCS[kg/m^2]	120.70
OMC[%]	15.5

Stabilization of Subgrade Soil with CPA

Atterberg Limit

CPA was used to stabilize the lateritic soil by mass from 4 to 12% interval. The results of the LL, PL and PI are presented in Figure 2. LL varies from 29.0 to 43.8%; and decreased from 42.20% for the sample soil to 29.0, 39.70, 39.12 and 38.80% for 0%CPA, 4%CPA, 8%CPA, 10%CPA and 12%CPA respectively. The decrease may

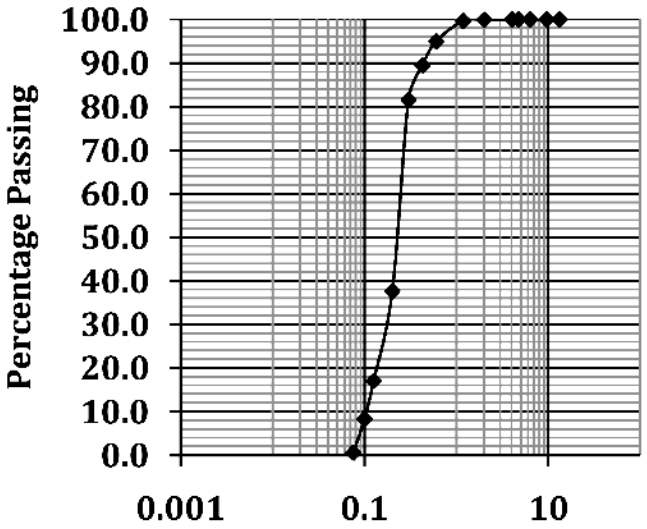

Fig. 2: Grain size distribution curve for tested soil.

be attributed to flocculation and agglomeration arising from cation exchange reactions in the additives reacted with ions of lower valence in the clay structure. This finding is in agreement with the findings reported by (Osinubi and Alhassan, 2008).PL varies from 14.0 to 33.3% and PI varies from 5.0 to 18.0%. At the point of adding 4% of CPA, the PI was 15.0%. From the results the PI at 0% (subgrade soil) was 18.70 and it later dropped to 15.0% at 4%, and there was gradual reduction from 8% to 12%. (Muntohar, 1999) established that a reduction in the PI of a stabilized soil is an indication of improvement. Consequently, the soil PI was improved with CPA percentages of 4 to 12%.

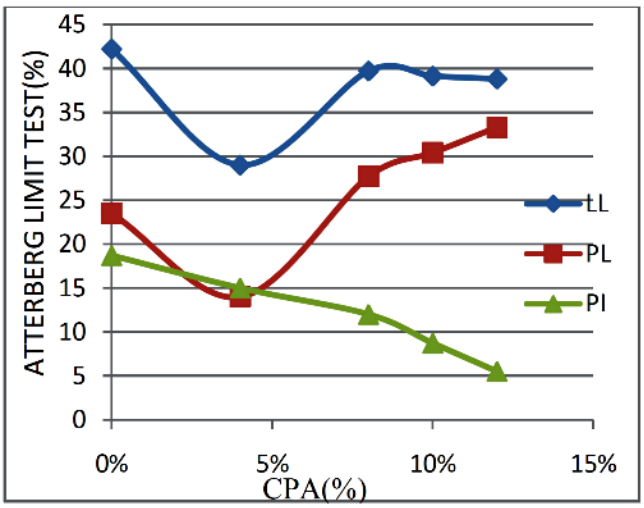

Fig. 3: Variation of Atterberg Limits of Stabilized soil with CPA.

Compaction Test Result

The Maximum Dry Density (MDD) with Optimum Moisture Content (OMC) obtained are as shown in Figures4and 5.The result shows that the addition of CPA led to increase of MDD at 4% and 8% stabilization with value of 1.80 and 1.88mg/m^3 receptively, after which there was continuous decrement in the MDD value. The OMC for the natural soil was 12.70, the addition of the CPA at 4% and 8% led to increase in the OMC and decrease at 10% downward 12%. The increase in MDD at 4% and 8%CPA recorded may be due to flocculation and agglomeration of the clay particles primarily due to cation exchange and addition the particles filling the voids within the soil matrix (Oriola and Moses, 2010).

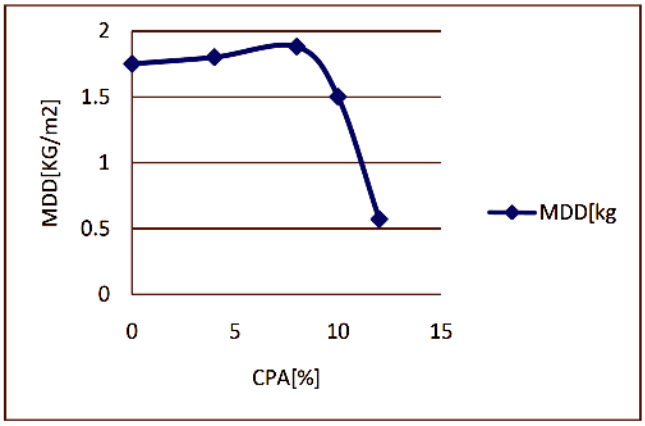

Fig. 4: Variation of Compaction test of Stabilized soil with CPA

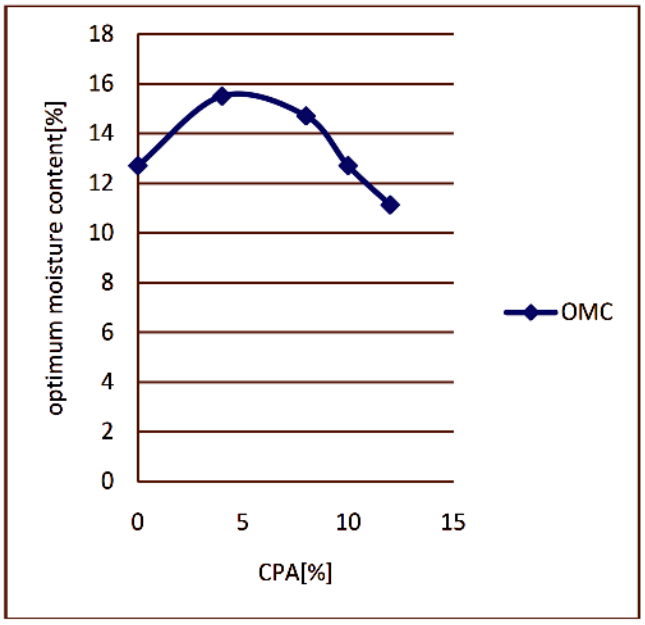

Fig. 5: CPA on the optimum moisture content of the samples

California Bearing Ratio

The CBR values obtained from the results of un-stabilized lateritic soil was 32%. The un-soaked CBR values obtained from the results of un-stabilized lateritic

soil is 32% while the optimum CBR values obtained for the stabilized lateritic soil is 46 % at 8% CPA.The Peak values of 46% at 8% CPA content, 35% at 4% CPA content, 35% at 10% CPA content, 36% at 12% CPA content and 32% at 0% CPA content as show in Figure 6. The reason for slight increment in strengths could be due to adequate amounts of CPA added to the sample. Those improvements in the CBR values satisfy the minimum requirements (7 and 30%) that qualify them as road construction materials for sub-grade respectively. (Nigerian General Specification, 1997).

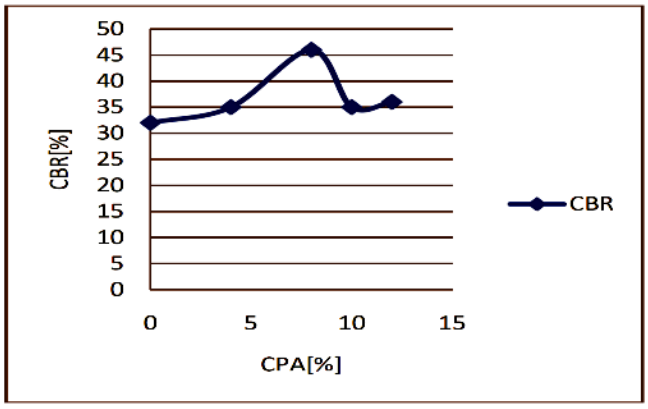

Fig. 6: CBR value versus CPA (%) Stabilization

Unconfined Compressive Strength (UCS) Test

The shear strengths of the stabilized soil samples increased compared to the un-stabilized soil sample. The results of the both stabilized and un-stabilized are shown at 0, 4, 8, 10 and 12% UCS values were 120.70, 575.50, 500,150 and 475kN/m^2 respectively. Addition of varying proportions of CPA improved compressive strength of natural soil beyond minimum standard requirement of 170kN/m^{2}for subgrade except for 10%CPA.The UCS increased considerably with the addition of CPA. These results further confirmed the stabilizing potentials of CPA on lateritic soil if added at the optimum level which is in line with the submission of (Bello *et al*. 2015).

Conclusion

Based on the results obtained from the study, the lateritic soil used was classified as A-6 according to the

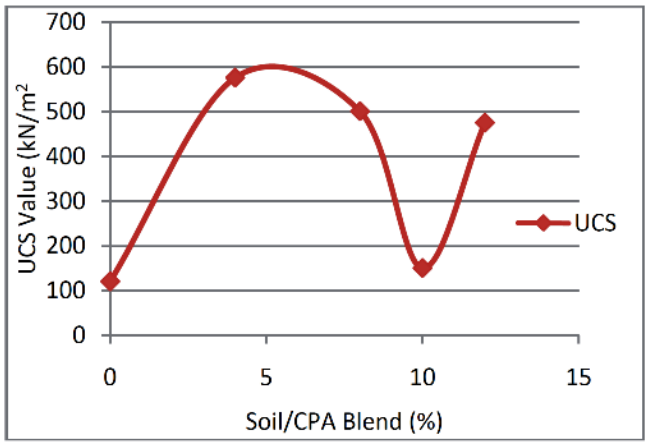

Fig. 7: UCS value versus CPA (%) Stabilization

AASHTO soil classification system (AASHTO, 1986).The percentages passing the no. 200 sieve was 37.60%. The liquid limit decreased from 42.20% for the sample soil to 29.0, 39.70, 39.12 and 38.80% for 0%CPA, 4%CPA, 8%CPA, 10%CPA and 12%CPA respectively while the plasticity index decrease from 18.78% at 0%CPA to a minimum value of 5.5% at 12%CPA. The MDD at 4% and 8% stabilization with the values of 1.80 and 1.88g/cm3 receptively, after which there is gradual reduction in the MDD value. The OMC for the natural soil is 12.70, at 0%, the addition of the CPA at 4% and 8% led to increase in the OMC and decrease at 10% downward 12%. The un-soaked CBR values obtained from the results of un-stabilized lateritic soil is 32% while the optimum CBR values obtained for the stabilized lateritic soil is 46 % at 8% CPA. The UCS value obtained at peaked was 575.50kN/m2 at 4%CPA. There is increase in the CBR; there is also increase in the shear strength of the lateritic soil due to the CPA that was added to the sample soil. The values obtained met the minimum specification by the Nigerian General Specification (1997) for un-soaked CBR for a sub grade and sub base material. It was shown that Cassava Peels Ash (CPA) improved the qualities of the soil sample by significantly reducing their plastic index. These reductions in plasticity index are indicators of soil improvement. The study therefore concluded at 8% Cassava Peels Ash (CPA) has the potential to effectively stabilize lateritic soils and can be used as a sub-grade and sub base materials in road construction.

References

Alhassan, M. (2008) Potential of rice husk ash for soil stabilization. AUJT;71(4):246- 250.

Amu, O.O and Adetuberu, A.A.(2010). Characteristics of bamboo leaf ash stabilization on lateritic soil in highway construction. International Journal of Engineering and Technology;2(4):212-219. .

Amu, O.O, Bamisaye, O.F, and Komolafe, I.A.(2011).The Suitability and Lime Stabilization requirement of Some Lateritic Soil Samples as Pavement. Int. Journal of Pure Applied Science and Technology;2 (1):29–46.

AASHTO.(1986). Standard Specifications for Transportation Materials and Method of Sampling and Testing.Amer. Assoc. State Highway and Transportation Officials, Washington, DC, USA.

ASTM (1992).Annual Book of StandardVol 04.80 American Society for Testing and Materials, Philadelphia.

Amu, O.O, Ogunniyi, S.A, and Oladeji, O.O.(2011) Geotechnical properties of lateritic soil stabilized with sugarcane straw ash.American Journal of Scientific and industrial Research. 2(2):323-331.

Amu,O.O, and Adetuberu, A.A.(2010). Characteristics of bamboo leaf ash stabilization on lateritic soil in highway construction. InternationalJournal of Engineering and Technology.2(4):212-219.

Bello, A.A, Joseph A.I and Hammed, A.(2015).Stabilization of Lateritic Soil with Cassava Peels Ash;*British Journal of Applied Science &Technology , 7(6): 642-650*

Bello, A.A and, Adegoke, C.W.(2013).Geotechnical characterization of abandoned dumpsite soil.ARPN Journal of Earth Sciences, ISSN 2505-403X, Asian Research Publishing Network.2(3):90-100. Available: http://www.arpnjournals.com.

Bello, A.A, Awogboro, O.S, and Oriaje, A.T.(2014). 'Influence of Compactive Efforts on Lateritic soil stabilized with Rice Hush Ash. International Journal of Applied Engineering.9(21):9639-9653.

Bello, A.A,Ige, J.A and, Ibitoye, G.I. (2014). Geotechnical properties of lateritic soil stabilized with cement-bamboo leaf ash admixtures.International Journal of Applied Engineering Research.;9(21):9639- 9653.

BS 1377.(1990). Methods of Testing Soil for Civil Engineering Purposes. British Standards Institute, London.

George, R.O and Karibo, P. (2014). Stabilization of Nigerian deltaic clay (Chikoko) with groundnut shell ash.International Journal of Engineering and Technology Research volume 2, No. 6, June, pg. 1 - 11, ISSN: 2327 – 0349..

Nigeria General Specification for Bridges and Road Works. Federal Ministry of Worksand Housing,Headquarters,Abuja,Nigeria.1997;11. (Revised).

Mitchell, J.K. (1976). Fundamentals of soil behavior, pp422.

Muntohar, A.S (1999). Behavior of Engineering Properties on the clay bedded with LRHA (LimeRice Husk Ash), Research Report Grant 1999, Yogyakarta, Indonesia.

Rahaman, M.A. (1988), "Recent Advances in the Study of the Basement Complex of Nigeria"

Sear LKA. Should you be using more PFA. Proc. Int. Conf. Cement Combination for Durable Concrete held at the University ofDundee, Scotland; 2005. UK. Lambe W.T.and Whiteman V. R., Soil Mechanics,

Oriola, F. and Moses, G. (2010).Groundnut shell Ash stabilization of Black Cotton soil.Electronic Journal of Geotechnical engineering, Vol. 15, pp415-428.

SI Version. New York: John Wiley and Sons.Inc; 1979.IS: 4031(Part 1):1996-Method of physical test for cement (Determination of fineness bydry sieving

IS: 4031(Part 1):1996-Method of physical test for cement (Determination of fineness by dry sieving).

Osinubi, K.J.(2001). Influence of compaction energy levels and delays on cement treated soil Technical Transaction of the Nigerian Society of Engineers 36 (4).

ISBN: 978-978-970-671-6

Proceedings of the 6th International Conference of the Nigerian Association for Engineering Geology and the Environment (NAEGE), Ibadan, Nigeria, 7th - 11th September, 2021 (Vol. 5), 2022.

Application of Geophysical Method in Investigating Road Failure Along Shendam Road, Lafia, North Central, Nigeria

Abimiku, Y.K., Olatinsu, O.B. and Fakeye, A.M.

Nigerian Building and Road Research Institute; [2]Physics Department, University of Lagos, Akoka.

Corresponding E-mail: **bonnke4lif@yahoo.com**

Abstract

A geophysical survey involving vertical electrical sounding (VES) techniques was carried out along Shendam road, Lafia,North Central, Nigeria, to unravel the subsurface geoelectric layers and the cause(s) of road failure in the study area. A total of twenty VES stations were established along two traverses beside the road pavement, with AB/2 varying from 1 to 100m andthe resistivity data were measured. The acquired data wereprocessed quantitatively through partial curve matching to delineate various layer resistivity and thickness and the plotted points were filter by WinResistSoftware and the geoelectric section were produced. The result shows that the major causes of road failure is due to the low resistive subsoil (>100Ωm) at shallow depth with mean value of 1.05m to the surface at VES 3, 4, 5, 7, 8, 11, 12, 13, 15, 16 and 18;which inferred the presence of clay or saturated sand, often less competent to support the stability of heavy vehicular movement, as result of constant expansion and contraction of clay material under varying weather condition, that lead to cracks and eventual collapse of the road. Other factor include poor drainage system for runoff water. Adequate recommendations are made to mitigate the cause.

Keywords*: Geoelectric, Resistivity, Subsoil, Traverse, Vertical electrical sounding.*

Introduction

Road failure has been a major problem in most part of the world, as many lives have been lost, injuries sustained, goods and property wasted due to road failure. The engineering structural failures common in the today's world include that of roads, bridges, buildings and dams. Road Failure is said to have occurred when there are unsatisfactory differences between expected and observed performance of a road after construction; the inability of a road to provide the primary objective for which it was constructed, as a result of discontinuity in the road pavement (Gerald, 1982).

Engineering structures are generally designed and constructed with long lifespans expectation, however, it has been observed over the years that the road often deteriorates before its designed age or after they are reconstructed or maintained. These pavement failures are often seen as cracks, depression, bulges and potholes on our roads which have adverse effect on both vehicles and the passengers (Rahaman, 1976; Aigbedion, 2007). Studies of past road failures showed some major causes of road failure as improper road usage, design error and construction problem (Adegoke-Anthony and Agada, 1987), use of inferior materials for road construction (Momoh et. al., 2008).

Factor leading to continued failure of road in Nigeria may be due to insufficient understanding of the characteristics and behaviour of substrates on which the roads are built and failure to consider the geomorphology and geology in the design of these roads (Ajayi, 1987; Adiat et al., 2009; Igwe, 2015), the presence of expansive clay/clay materials (such as montmorillonite, chlorite, halloysite, etc.) at the top soil and/or subsoil (Meshida, 1987; Oladapo, et al., 2008).

Other reason may arise from natural factor relating to tectonic activities that take place within the earth, such as earthquake, tremor, bedrock depressions and presence of undetected linear features, such as fractures and rock boundaries (Akintorinwa et al., 2010;Ibitomi et al., 2014; Egbeyale et al., 2019).

Since every engineering structure is located on geological earth materials, experts in geology and geophysics always stressed out that insufficient information on the nature of soil beneath the earth before construction as a main factor leading incessant failure(Momoh et al., 2008; Ibitomi et al., 2014). Therefore, it has become imperative to understand the shrinkage properties of the soil as it is very important in solving engineering problems typically connected with the construction of foundation of buildings, dams, bridges or highways. (Egwuonwu and Sule, 2012, Adenika et al., 2018). As a result of this, geophysical survey techniques is often implored, to delineate subsurface sequence and identify geological structures, to enhance easy characterization of the subsurface soil and determination of thickness and depth required for the design of civil engineering foundation, which is highly relevant due to its non-invasive approach, relatively low cost and time-saving advantage (Emujakporue, 2012).

This study was carried out to characterize the subsurface condition at failed portion of Shendam road and to unravel the cause of road pavement failure in the study area.

Location and Geology of the Study Site

The site is located North-West of Lafia, on an express road leading to Shendam LGA in Plateau State.It lies between latitude 8º 28' to 8º 36' N and longitude 8º 40' to 8º 50' Ewhich falls within the Middle Benue Trough Basin. It is of fairly plain terrains, with rocky and undulating highlands to average height of about 180m above sea level. The vegetation is Guinea Savannah, with distinct wet and dry season, having mean annual rainfall of about 1,357mm and annual temperature of 17^0C and 35^0C for a very cold and very hot day respectively (Nigerian Meteorological Agency Lafia, 2012). The state is made up of 60% Basement complex rocks and the 40% sedimentary rocks of the Benue Trough (Obaje, 2006).

The study area is laid uncomfortably on basement complex terrain bonded by lafiaformation (see figure 1), the Cretaceous sediment of the Middle Benue Trough, deposited under continental fluviatile condition in the Maastrichtian and lies partly on the Awgu formation which was reported to have been deposited during the Late Turonian transgression, early Coniacian and terminated in the early Santonian(Obaje, 2006). This deposition marks the end of marine sedimentation in this part of the Benue Trough. Thelithologies include black carbonaceous shales, sandstones, siltstones, local coal seams, clays and claystones (Offodile, 2002).

Electrical Resistivity Method

Electrical resistivity method is basically used to measure and record the resistivity of subsurface material. It is a survey that is carried out to present the image of electrical characteristics of the subsurface earth by passing anartificial generated current across arrays of electrodes stationed at calculated distance on the ground and measuring the associated voltage (Kearey et al., 2002). The basis of electrical resistivity theory is the Ohm's law, which established the relationship between the resistance (R), the potential difference (V) and the current (I) as:

$$V = IP \qquad R = V/I$$

Since the current is known as well as the voltage, it is possible to determine the apparent resistivity of the surface (Telford *et al*., 1976). An equation for the apparent resistivity in terms of applied current distribution and potential is calculated by dividing the measured potential difference (V) by the input current (I) and multiplying by a geometric factor (K) of the array being used.

$$\rho_a = \left(V/I\right) * K \qquad \rho_a = K * R$$

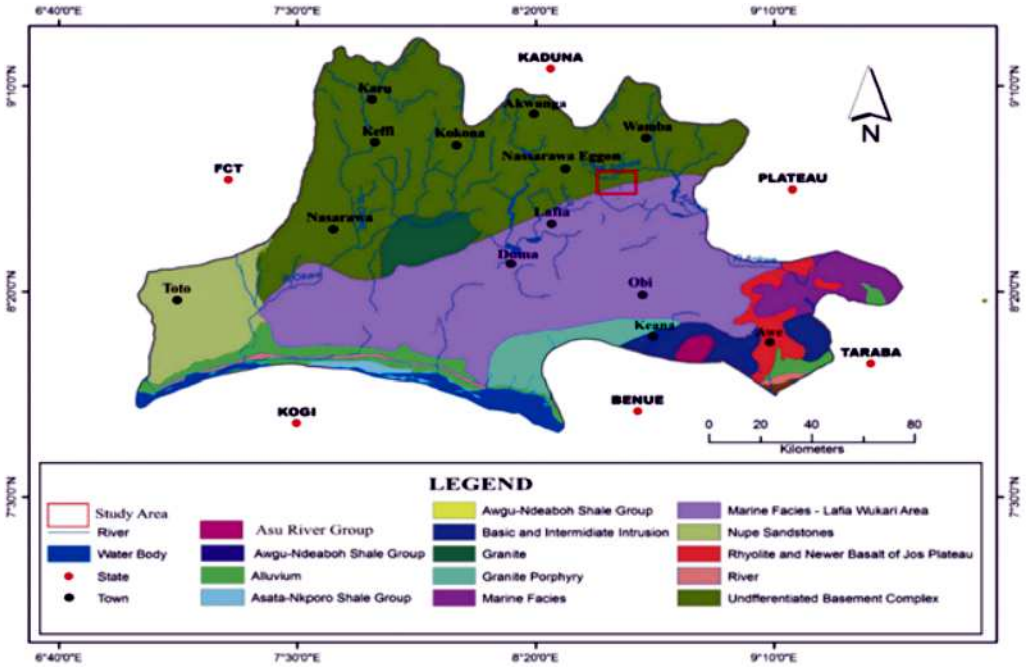

Fig. 1: Geological Map of Nasarawa State showing the study area (adapted from Obaje, 2006).

Materials and Method

The earth resistivity measurement was carried out using Ohmega resistivity meter and Global Positioning System (GPS) was used to measure the coordinates and elevations of each VES point. Two (2) traverse were established beside the road pavement in the study area with Ten (10) Vertical Electrical Sounding (VES) stations occupied along each of this traverse (see figure 2), using Schlumberger electrode array with half current electrode spacing (AB/2) varied from 1 to 100m and half potential electrode spacing (MN/2) varied from 0.25m to 5m. The data for each electrode movement were recorded as resistance (R), which was then multiplied by a geometric factor (K) to give the apparent resistivity (ρ_a).

The VES data were interpreted by plotting apparent resistivity values against the half current electrode spacing (AB/2) on a bi-logarithmic graph, to generate various layers resistivity and thickness and the obtained results were iterate by a computer basedprogram Win Resist version 1.0 to filter the plotted points and smoothen the curveand Surfer 12 © software was used to produce the geoelectric section of the interpreted VES data.

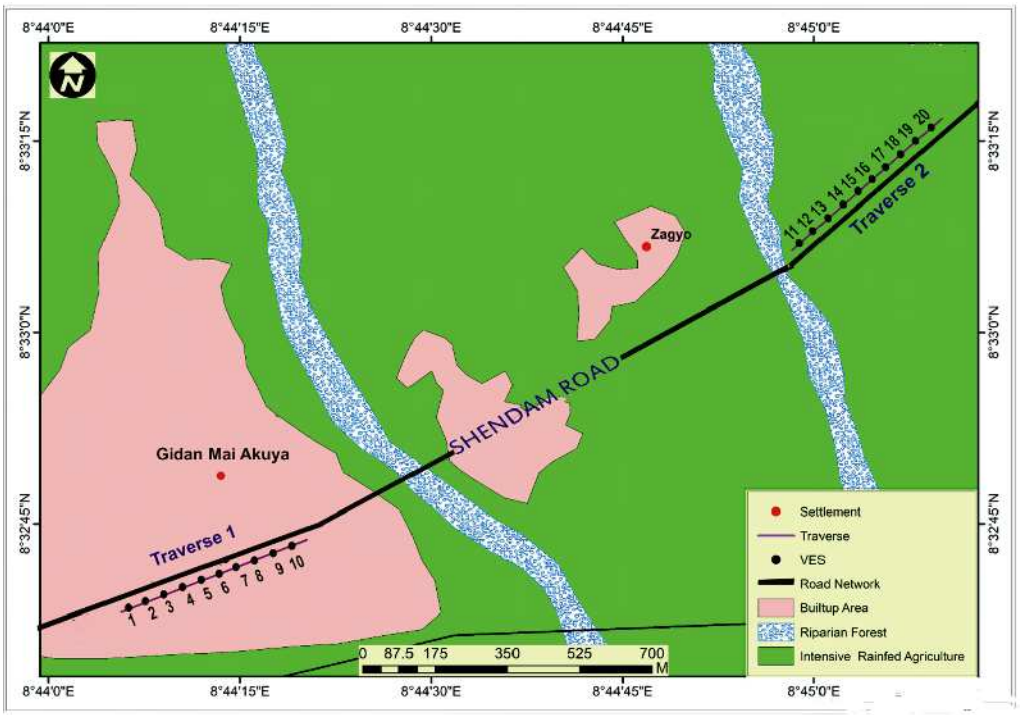

Fig. 2: Basemap of the study area.

Result and Discussion

Three (3) resistivity curve types were obtained from the study area, which are the H, QH and QQH. QH curve is the predominant one, constituting 80%, while the H and QQH types constitute 15% and 5% respectively (see figure 3).

Figure 4a and 4b shows geoelectric section for traverse 1 (VES 1 to 10) and traverse 2 (VES 11 to 20)repectively. It reveals three and four geologic layers which varies from topsoil, weathered layer, sandy clay and fresh basement.

From the geoelectric section, VES 1, 2, 6, 9, 10, 14, 17, 19 and 20,are founded on lateritic subgrade soilwith

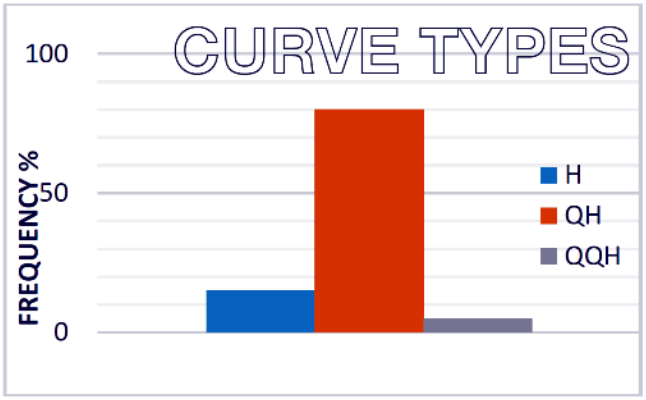

Fig. 3: Histogram of curves typefound in the study area

resistivity value range from 273.4 – 1143.6Ωm, at depth range of 0 – 1.2m for traverse 1 and resistivity value

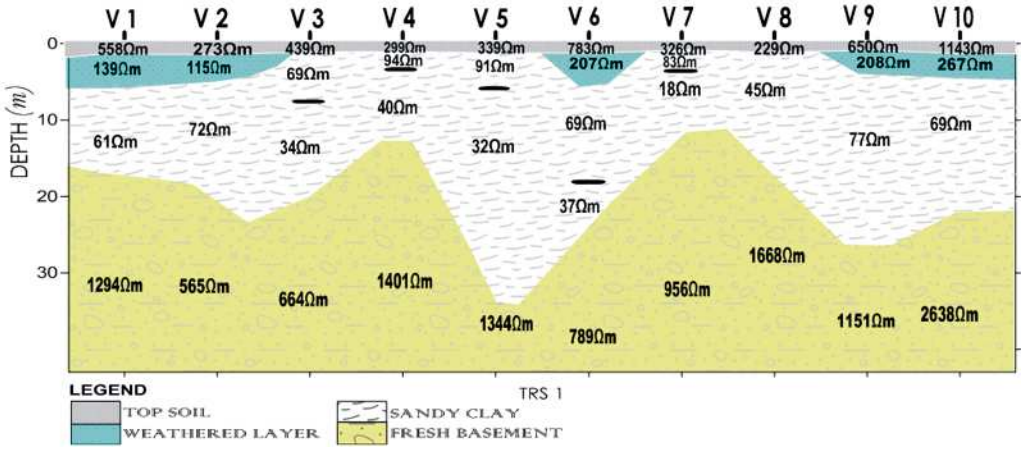

Fig. 4a: Geoelectric Section for Traverse 1

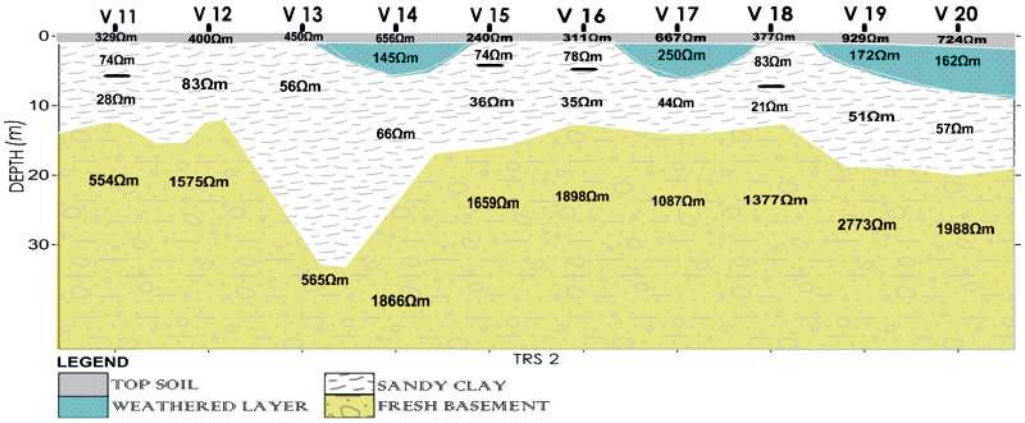

Fig. 4b: Geoelectric Section for Traverse 2

range from 556.4 – 929.3Ωm, at depth range of 0 – 1.7m for traverse 2.

The subsoil (weathered layer) resistivity value ranges from 115.6 – 267.0Ωm, at depth range of 0.8 – 1.3mfor traverse 1 and 145.7 – 250.7Ωm at depth range of 0.9 – 1.8 m for traverse 2,which infer a layer characterized by constituents of weathered materials typically of sand.

The third geologic unit characterized sandy clay layer, having resistivity value ranges from 37.3 – 77.8; 44.5 – 66.3Ωm at depth range of 4.5 - 6.8m; 5.6 - 8.8m for traverse 1 and 2 respectively. The clay material in this layer has less impact on the road pavement due its extensive depth and high resistive top soil and subsoil layer along these VES points.The basement resistivity values range from 564.8 to 2637.6Ωm and 1087 to 2773Ωm with an infinite thickness but, the depth to the bedrock ranges between 12.4 to 21.2m and 11.2 to 18.5m for traverse 1 and 2 respectively. These VES points form the stable portion of the road due to the high resistive top and subsoil at these VES points.

At VES 3, 4, 5, 7, 8, 11, 12, 13, 15, 16 and 18,the road is characterized by thin topsoil subsumed in the subsoil in many places due to its thickness, with resistivity value range from 229.1 – 439.7Ωm, at the depth range 0 – 1.1m for traverse 1 and resistivity value ranges between 240.4 – 450.1Ωm, at depth range of 0 – 1.2m for traverse 2.

The subsoil and the third layer resistivity value ranges from 68.6 – 93.8 Ωm, at depth range of 0.7 – 1.3m for the subsoil and resistivity value between 18.4 – 34.1Ωm, at the depth range of 3.4 – 15.7m for thethird layerfor traverse 1 and for traverse 2, the resistivity value range from56.2 – 83.2Ωm, at depth range of 0.9 – 1.2m for the subsoil andranges between21.3 – 36.1Ωm at depth range of 4.6 – 14.5mfor the third layer. The resistivity value of the subsoil layer less than 100Ωm to the top soil at a shallow depth,between 0.7-1.3m atVES 3, 4, 5, 7 and 8 (for traverse 1) and between 0.9-1.2m atVES 11, 12, 13, 15, 16 and 18 (for traverse 2) infer layers characterized by constituents of weathered materials, typically of saturated sand/clay that absorbs and losses

water at varying season, caused them to swell and shrink which lead to cracks, potholes and ultimately collapse of the road pavement, under applied wheel load stress.

The basement resistivity values range from 664.2 - 1668.6Ωm and 554.4 - 1898.6Ωm with an infinite thickness but, the depth to the bedrock ranges from 11.9 - 28.1m and 14.5 - 33.6m for traverse 1 and 2 respectively. The bedrock topography is uneven, with basement depression experience at VES 5 and 13, this can also act as zones of weakness that enhance accumulation and percolation of water which lead to pavement failure.

Conclusions

Electrical Resistivity methods has been used to ascertain the cause(s) of incessant road failure on a portion of Shendam road, Lafia, North Central Nigeria. The result obtained from the study reveals the major cause of pavement failure as the clayey nature of the subsoil at shallow depth beneath the subsurface, which is impermeable as a result of poor pores connectivity and its elastic properties to absorb water and swell during rainy season and shrink during dry season; as this seasonal volumetric changes cause the soil to easily deforms at the exertion of stress or pressure from heavy vehicular movement and the presence of near surface features such as basement depression at the bedrock at some VES point, also poise threat to the integrity of subsurface as it can lead to water accumulation and percolation, which may result to pavement failure. Moreover, some region of the road pavement is being washed off by water causing erosion which weaken the pavement.

Recommendations

In order to prevent incessant occurrence of road pavement failure in this area, it is recommended that the subsoil of weak region should be excavated to a reasonable depth between 1.3 – 4.6m, where the soil has sufficient strength and replace with a competent road fill material or by using chemical stabilizer to increase the soil bearing capacity and adequate drainage system should be provided for runoff water. Detailed geophysical survey shouldalso be carried out on other similar road before construction or rehabilitation, to determine the weak zone and ensure long term stability and integrity of the road.

References

Adegoke-Anthony, W.C. and Agada, O.A., Oladapo (2008):Geophysical investigation of a road failure in the basement complex area of southwestern Nigeria. Research Journal of Applied Science. Pg 102-122

Adenika, I.C., Emmanuel, A.A., Musa, O.A. and Adebiyi S.A., (2018). Application of Geophysical Approach to highway pavement failure; a case study from basement complex terrain southwestern, Nigeria. Inernational Journal of Geo-Engineering, 9(8): p25-47.

Adiat, K.A.N, Adelusi, A.O. and Ayuk, M.A., (2009): Relevance of geophysics in road failures investigation in a typical Basement Complex of Southwestern Nigeria. Pacific Journal of Science and Technology Vol. 5(1): 528–539.

Aigbedion, I., (2007): Geophysical investigation of road failure using electromagnetic profiles along Opoji, Uwenlenbo and Illeh in Ekpoma, Nigeria. Middle East Journal of Scientific Research Vol. 2(3–4): 111–115.

Ajayi, L. A., (1987): "Thoughts on Road Failures in Nigeria". Nigerian EngineerVol. 22(1): 10-17.

Egbeyale G.B., Ogunseye, T.T. and Ozegin K.O., (2019). Geophysical investigation of building foundation in part of Ilorin, North Central Nigeria. Journal of Physics: Conference Series 1299 012064.

Egwuonwu G.N., and Sule. O., (2012): "Geophysical Investigation of Foundation Failure of a Leaning Superstructure in Zaria Area, Northern Nigeria," Research Journal in Engineering and Applied Sciences, Vol. 1(2), 110-116.

Emujakporue, O.G., (2012). Geophysical investigation of the causes of highway failures in Niger Delta Sedimentary Basin (A case study of the Eastern part of East-West road), Nigeria. Scientia Africana 11(1): p143–152.

Gerald A. L., (1982): Discussion of "Investigation of Failures". Journal of Geotechnical Engineering. p110(1).

Ibitomi M. A., Fatoye F.B., and Onsachi J.M., (2014). Pavement failure on a portion of Okene-Lokoja Highway, North Central, Nigeria. The International Institute for Science, Technology and Education (IISTE). 4(13): p22-32.

Igwe, O. (2015). The causes and mechanisms of rain-induced highway and pavement collapse in Obolo-eke, Southeast Nigeria. Arabian Journal of Geosciences, 811, 9845-9855.

Kearey, P., Brooks, M. and Hill, I., (2013). "An Introduction to Geophysical Exploration". John Wiley & Sons. Pg 262.

Loke, M.H. (2000): "Electrical Imaging Surveys for Environmental and Engineering Studies". (A Practical Guide to 2-D and 3-D Surveys). Manual, Copyright (1997, 1999).

Meshida, E.A. (1987): The relationship between the geology and the lateritic engineering soils in the Northern Environs of Akure, Nigeria. Bulletin of the International Association of Engineering Geology, Vol. 35: 65–69.

Momoh, L.O., Akintorinwa, O.J. and Olorunfemi, M.O. (2008): Geophysical investigation of highway failure. A case study from the Basement Complex Terrain of South-western Nigeria. Journal of Applied Sciences Research, Vol. 4(6): 637–648.

*Obaje N.G. (2006): "*Geology and Mineral Resources of Nasarawa State: An Investor's Guide". *Publisher, Department of Geology and Mining, Faculty of Natural and Applied Sciences, Nasarawa State University. p3-9.*

Offodile, M.E. (2002): A mineral survey of the Cretaceous of the Benue Valley, Nigeria. Cretaceous. Res Vol. 1: 101–124.

Oladapo, M.I., Olorunfemi, M.O. and Ojo, J.S. (2008): Geophysical investigation of road failures in the Basement Complex area of South-western Nigeria. Research Journal of Applied Sciences. Vol. 3(2): 103 – 112.

Rahaman, M.A. (1988): "Recent Advances in the study of the Basement Complex of Nigeria". Kogbe, C.A. (ed.), Geological Survey of Nigeria, Elizabethan Publishing Company, p11 – 41.

ISBN: 978-978-970-671-6

Proceedings of the 6th International Conference of the Nigerian Association for Engineering Geology and the Environment (NAEGE), Ibadan, Nigeria, 7th - 11th September, 2021 (Vol. 5), 2022.

Investigation of Aquifer Vulnerability and Pollution Index around Industrial Area in Ilorin, Northcentral Nigeria

Ibrahim, K.O.[1], Yusuf, M.A.[1] and Purchase, M.W.[2]

[1]Faculty of Physical Sciences, Department of Geology and Mineral Sciences, University of Ilorin, Ilorin, Nigeria

[2]Faculty of Natural & Agricultural Sciences, Department of Geology, University of the Free State, Bloemfontein, South Africa

Corresponding E-mail: **ibrahim.ko@unilorin.edu.ng**

Abstract

Urban pollution due to increased industrialization has become a major concern in recent time. In most cases, hazardous wastes from industries infiltrate groundwater especially in unconfined alluvial aquifer if proper precautions are not taken. This study used GOD model to investigate aquifer vulnerability around industrial area in Ilorin, North-central Nigeria. Heavy metals (Cd, Cr, Zn, Pb, Fe, Ni, Mn, Cu, Co) were also determined from groundwater in study area using metal pollution index (MPI) to validate the GOD model. Three main vulnerability zones were recognized in the study area and these are: low vulnerability zones with GOD index values ranging from0.22 to 0.26 and moderate vulnerability zones having GOD index value of 0.48 while high vulnerability zones possess GOD index values ranging from 0.56 to 0.64. The pollution index show that the area is highly polluted with respect to (Cd, Cr, Pb, Fe, Ni, Mn, Cu and Co) and lightly polluted with Zn. The sources of pollution in the study area areattributed to industrial effluent discharges. There is urgent need for measures to mitigate further groundwater pollution and protection of aquifer in the study area.

Keywords*: Aquifer; Vulnerability; Heavy-Metals; Pollution*

Introduction

Groundwater constitutes the freshwater available for domestic, industrial and agricultural use (Mirzavand and Ghazavi, 2015). The adequacy of groundwater resources, both in quality and quantity is important for socio-economic development of an area (Majolagbe et.al, 2016). Both groundwater and aquifer are under intense threats from environmental influences and pollutions such as leachates from domestic, industrial wastes (Idowu et al., 2016) and various land use configuration such as application of chemicals that result to groundwater pollution (Adesola et al., 2016; Babarinde and Onyiaocha, 2016) and these pollutants possess some heavy metals that are harmful to the environment with negative impact on water.

The vulnerability of groundwater to pollution could be defined as a tendency of groundwater in an area to be contaminated or polluted (Majolagbe et al., 2016). Study of aquifer vulnerability to pollution assist to understand the distribution of the highly vulnerable areas, in which there are possible pollution occurrences either now or in the near future (Ibrahim et al., 2017). Aquifer vulnerability connotes that different parts of an aquifer may offer different degrees of protection to the groundwater contained in them (Recinos et. al., 2014). For instance, in highly porous alluvial soils such as sand and gravels are considered to be very good aquifers with high yield values, but are the most vulnerable and are unprotected from surface pollution if no proper protection measures are put in place (Ibrahim et al., 2017).

Various methods have been developed for the assessment and evaluation of groundwater vulnerability to contamination from surface pollution. The DRASTIC model (Aller et al., 1987) was first developed for the US Environmental Protection Agency. Following DRASTIC are other methods such as AVI (Van Stempvoort et al., 1993), COP (Vias et al., 2006), EPIK (Doerfliger et al., 1999), GOD (Foster, 1988), SINTACS (Civita, 2000), VULK (Sinreich et al., 2007) and many more.

The aquifer system in the study area is primarily unconfined aquifer, porous and permeable, therefore, there is possibility of contaminants to infiltrate through the soil into the shallow watertable in the study area. This study was carried out to evaluate the performance of GOD model in determining surficial aquifer vulnerability in an industrial area. The GOD model was validated with heavy metals using pollution index.

Location of the Study Area

The study area is situated within latitude 8^0 27' 03"N, 8^0 29' 02" N and longitude 4^0 31' 45" E, 4^0 35'30"E (Ilorin Topographical Sheet 223 N.W) with about 16km. The area is in the intermediate zone between semi-arid in the

north and sub-humid climate in the southdistance as shown in Fig. 1, hence characterized by two distinct seasons, that is, the wet season which starts in late march and ends in the mid of October, while cold and dry weather due to influence of Harmattan is observed in the months of December and January.

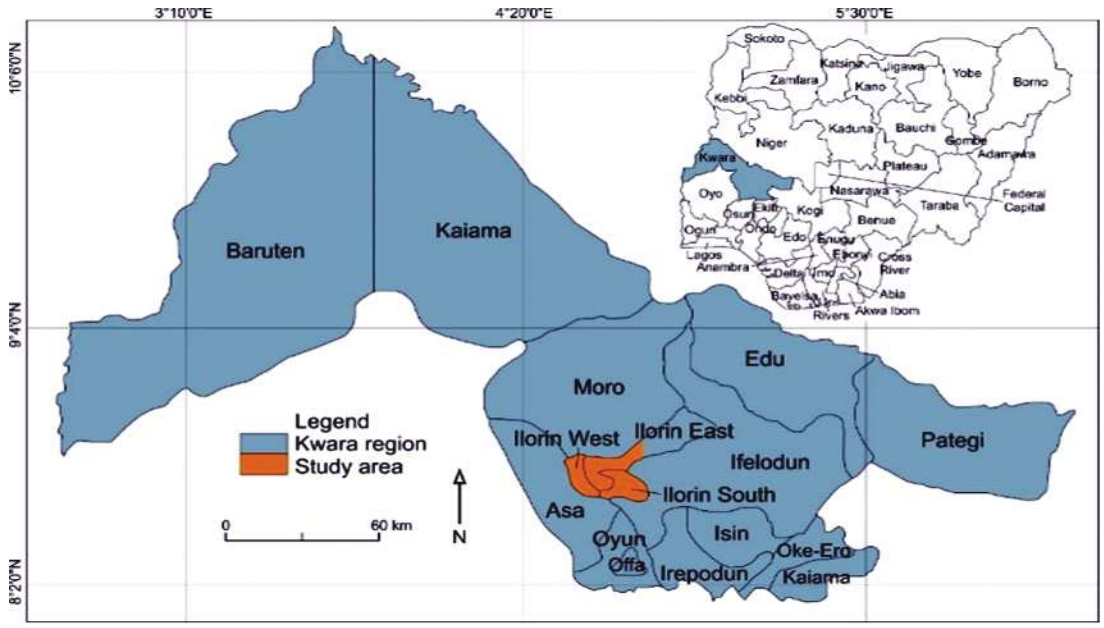

Fig. 1: Map of Kwara state showing study area.

Geology and Hydrogeological Settings of the Study Area

The study area is situated on the Precambrian Basement Complex rocks that include granite, granitic gneiss and migmatite (Alao and Ige, 2003; Omotoso et al., 2011). The rocks form part of regional northwestern Island running northwest – southeast parallel to the River Niger (Annor and Olasehinde, 1996). These represent the deeper fractured aquifers which is partly overlain by a shallow porous aquifer (Alao and Ige, 2003). Moreover, Omotoso et al., 2011 further reported that the gneisses are foliated with light and dark bands and the main minerals are suspected to be quartz, feldspar and mica as observed from the petrographic analysis of rock samples. Quartzite veins cut across one another as observed from the field mapping. Structurally, lineations, foliations, joints, fractures and folds are the main features observed on the rocks. Fig. 2 presents the geological map of Nigeria showing the study area.

The surficial aquifer in the study area is mainly of alluvial deposits which composed primarily of sand and gravel while clayey materials are found in some few places. The depth of these surficial aquifers in the study area ranges between 5.0 m to 11.2m as shown in Table 1.

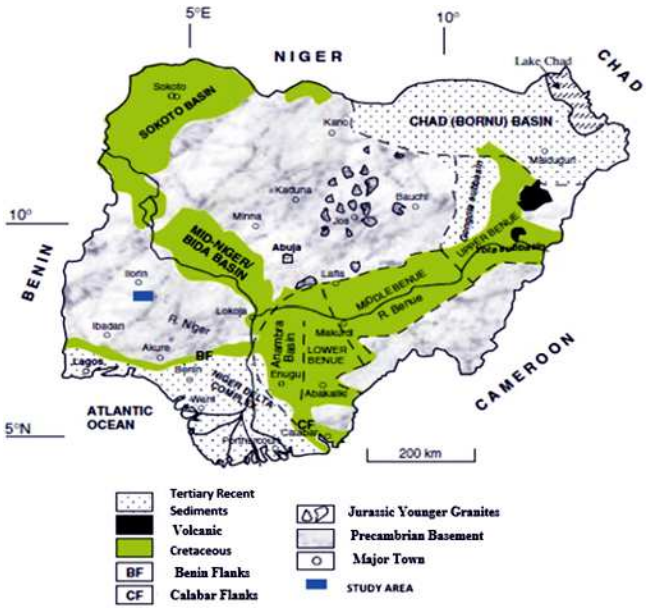

Fig. 2: Geological map of Nigeria showing study area (After Obaje and Abba, 1996)

Methodology

The GOD method was applied to determine aquifer vulnerability in study area. Samples were generated from twenty (20) wells locations based on industrial activities in the area as shown in figure 3. The GOD

Table 1: Database for surficial aquifer vulnerability assessment in study area

Well No.	X	Y	Groundwater occurrence	Overall lithology of aquifer	Depth of groundwater	G	O	D	GOD Index
1	8° 29' 02''	4° 33' 43''	Semi-Confined	Clayey sand	10.2	0.4	0.8	0.7	0.22
2	8° 28' 53''	4° 33' 57''	Unconfined	Sand	5.3	1.0	0.6	0.8	0.48
3	8° 28' 45''	4° 33' 28''	Unconfined	Sandy gravel	5	1.0	0.7	0.9	0.63
4	8° 28' 41''	4° 33' 39''	Unconfined	Sandy clay	6	1.0	0.6	0.9	0.61
5	8° 28' 03''	4° 33' 31''	Semi-Confined	Clayey sand	10.7	0.4	0.8	0.7	0.22
6	8° 28' 19''	4° 33' 44''	Unconfined	Sandy clay	6.3	1.0	0.6	0.9	0.61
7	8° 28' 15''	4° 33' 48''	Semi-Confined	Clayey sand	8.6	0.4	0.8	0.8	0.26
8	8° 28' 08''	4° 33' 60''	Unconfined	Gravel sand	6.7	1.0	0.8	0.8	0.64
9	8° 27' 54''	4° 33' 46''	Unconfined	Sand	5.2	1.0	0.6	0.8	0.48
10	8° 27' 34''	4° 33' 28''	Unconfined	Sandy clay	5.7	1.0	0.6	0.9	0.62
11	8° 26' 46''	4° 33' 35''	Semi-Confined	Clayey sand	11.2	0.4	0.8	0.7	0.22
12	8° 27' 08''	4° 32' 60''	Unconfined	Sandy gravel	7.9	1.0	0.7	0.8	0.56
13	8° 27' 13''	4° 32' 57''	Unconfined	Sand	8.6	1.0	0.6	0.9	0.62
14	8° 27' 23''	4° 32' 14''	Unconfined	Gravel sand	6.9	1.0	0.8	0.8	0.64
15	8° 27' 26''	4° 32' 01''	Semi-Confined	Clayey sand	10.8	0.4	0.8	0.7	0.22
16	8° 27' 33''	4° 31' 58''	Unconfined	Gravel sand	7.2	1.0	0.8	0.8	0.64
17	8° 27' 03''	4° 31' 47''	Semi-Confined	Clayey sand	7.9	0.4	0.8	0.8	0.26
18	8° 26' 53''	4° 31' 45''	Unconfined	Gravel sand	5.3	1.0	0.8	0.8	0.64
19	8° 27' 35''	4° 33' 05''	Unconfined	Sandy gravel	6.6	1.0	0.7	0.8	0.56
20	8° 28' 32''	4° 33' 12''	Unconfined	Gravel sand	5.6	1.0	0.8	0.8	0.64

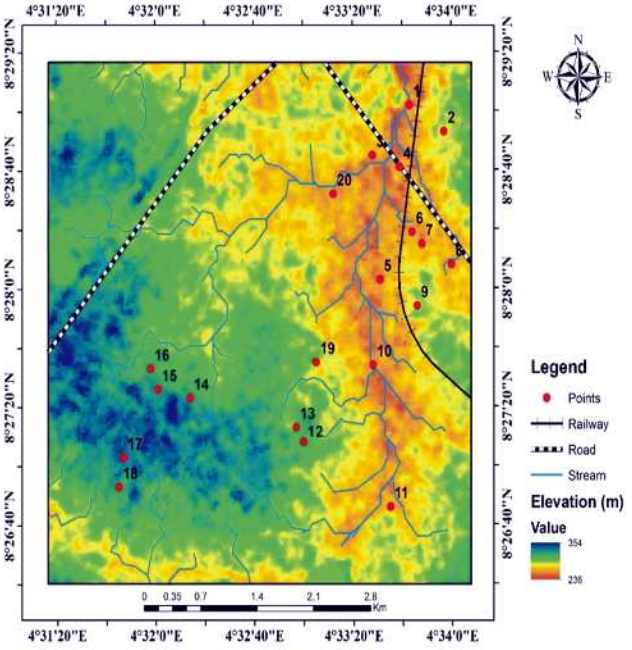

Fig. 3: Map of study area showing sampling points.

model is based on multiplication of three input parameters in the area namely: Mode of groundwateroccurrence (G); Overlying lithology (O) and Depth to water table (D).

To validate GOD model, groundwater samples were collected based on industrial activities locations in the study area which include pharmaceutical, soap and detergent, flour mill amongst others to represent the conditions of groundwater in each location. The water samples were analysed for heavy metals (Cd, Cr, Zn, Pb, Fe, Ni, Mn, Cu and Co) at the Kwara state ministry of water resources in Ilorin, Nigeria.

The chart in figure 4 shows the evaluation procedure using GOD model. The interpretation of GOD model classified aquifer vulnerability into neglect, low, moderate, high and extreme high vulnerability to contamination. The GIS integration of the collected field data was carried out using ArcView platform by Environmental Systems Research Institute (ESRI, 1999) to generate a vulnerability map for the study area.

Results and Discussions

The data generated from GOD model are presented in Table 1 and Table 2. These data include groundwater occurrence (G); aquifer lithology (O) and depth of groundwater (D). The surficial aquifer vulnerability of the study area is classified into three (3) zones: low vulnerability zone, moderate vulnerability zone and high vulnerability zone (figure 5). The low vulnerability zones have GOD index values ranging from0.22 to 0.26

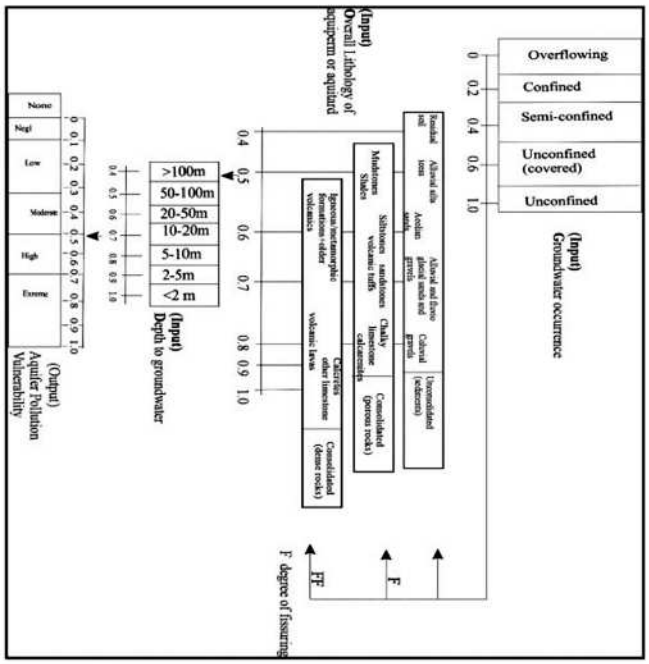

Fig. 4: GOD Model for evaluation of aquifer vulnerability index (Foster, 1988)

Table 2: Classification of aquifer vulnerability in study area

Well No.	X	Y	Aquifer Vulnerability
1	8^0 29' 02"	4^0 33' 43"	Low
2	8^0 28' 53"	4^0 33' 57"	Moderate
3	8^0 28' 45"	4^0 33' 28"	High
4	8^0 28' 41"	4^0 33' 39"	High
5	8^0 28' 03"	4^0 33' 31"	Low
6	8^0 28' 19"	4^0 33' 44"	High
7	8^0 28' 15"	4^0 33' 48"	Low
8	8^0 28' 08"	4^0 33' 60"	High
9	8^0 27' 54"	4^0 33' 46"	Moderate
10	8^0 27' 34"	4^0 33' 28"	High
11	8^0 26' 46"	4^0 33' 35"	Low
12	8^0 27' 08"	4^0 32' 60"	High
13	8^0 27' 13"	4^0 32' 57"	High
14	8^0 27' 23"	4^0 32' 14"	High
15	8^0 27' 26"	4^0 32' 01"	Low
16	8^0 27' 33"	4^0 32' 58"	High
17	8^0 27' 03"	4^0 32' 47"	Low
18	8^0 27' 43"	4^0 32' 35"	High
19	8^0 27' 35"	4^0 33' 05"	High
20	8^0 28' 32"	4^0 33' 12"	High

and consists predominantly of clayey sand. The moderate vulnerability zones possess GOD index value of 0.48 which compose of sands and sandy - clay while high vulnerability zones have GOD index values ranging from 0.56 to 0.64 with mainly of sandy-gravel and gravel-sand. The vulnerability map of the surficial aquifer in the study is presented in Figure 4.

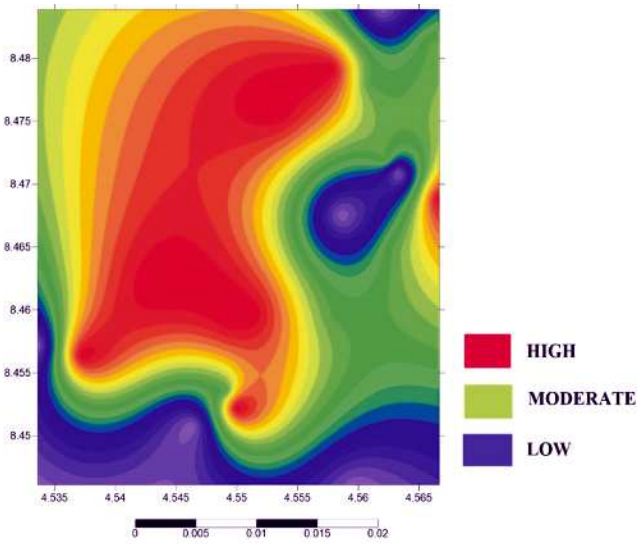

Fig. 5: A produced vulnerability map for study area

The statistical summaryof heavy metals concentrations in groundwater in the study area is presented in Table 3.

Table 3: A statistical summary of heavy metals concentrations (mg/l) in the study area

S/N	Parameters	Min.	Max.	Average mean
1	Cd	0.03	2.31	0.45
2	Cr	0.10	3.10	1.06
3	Zn	0.04	5.70	1.07
4	Pb	0.10	50.5	13.3
5	Fe	11.0	79.0	40.2
6	Ni	0.03	5.10	1.28
7	Mn	2.00	88.0	25.0
8	Cu	5.30	105	51.7
9	Co	0.11	10.4	4.08

The groundwater pollution index in study area was determined using metal pollution index (MPI) method as shown in Table 4 which used to indicate the impact of metallic parameters on the overall quality of the water (Udoh and Amadi, 2020). MPI values also indicates the relative impact of heavy metals on the quality of water in the study area. The higher the concentration of a metal when compared to its maximum permissible level, the poorer the quality of the water (Taylor and McLennan, 1995).

Equations

The MPI formula is expressed as follows:

$$MPI = \sum_{i=1}^{n} \left(\frac{C_i}{(MAC)_i} \right) \quad \text{.....(1)}$$

Where C_i is the mean concentration
MAC is the maximum allowable concentration
There are generally five (5) groups of MPI namely as:
MPI < 0.01 = Very lightly polluted
0.01– 1.0 = Lightly polluted
1.0 – 5.0 = Moderately polluted
5.0 – 10.0 = Highly polluted
> 10.0 = Very highly polluted

The computed metal pollution index for the groundwater in the area as presented in Table 4 ranked the degree of metallic pollution from very highly polluted (Cd, Cr, Pb, Fe, Ni, Mn, Cu and Co) to lightly polluted (Zn) and the possible sources of the pollution in the area are from industrial effluent of soap and detergent, pharmaceuticals, bottling companies among others.

Table 4: Computed metal pollution index (MPI) for groundwater in study area

Parameter (Mg/l)	*Ci*	*MACi* NSDWQ (2017)	MPI Value	Rating
Cd	0.45	0.003	150	Very-highpolluted
Cr	1.06	0.05	21.0	Very-high polluted
Zn	1.07	3.00	0.36	Lightly polluted
Pb	13.3	0.01	1330	Very-highly polluted
Fe	40.2	0.30	134	Very-high polluted
Ni	1.28	0.02	64	Very-highly polluted
Mn	25.0	0.20	125	Very-highly polluted
Cu	51.7	1.00	51.7	Very-high polluted
Co	4.08	0.02	204	Very-high polluted

Conclusion

This study shows that most of the locations in the study area are prone to pollution. The validation of GOD method using a metal pollution indexclassified the study area to be very highly polluted to lightly polluted. Possible sources of groundwater pollution in the study area include industrial effluent of soap and detergent, pharmaceuticals and bottling companies which are located in the study area. Continuous monitoring of groundwater pollution in the study area is recommended to reduce future pollution.

References

Adesola, B., Ogundipe, K., Sangosanya, K.T., Akintola, B.D., Oluwa, A. and Hassan, E. (2016). Comparative study on the biosorption of Pb(II), Cd(II) and Zn(II) using Lemon grass (Cymbopogon citratus). Kinetics, isotherms and thermodynamics. Chemistry International, Vol. 2: 89 – 102

Alao, D.A. and Ige, O.O. (2003). Preliminary assessment of pollution of Asa river in Ilorin metropolis using physico-chemical indices. Water resources - Journal of the Nigerian Association of Hydrogeologists (NAH),Vol. 14:25-30

Aller, L., Bennett, T., Lehr, J., Petty, R. and Hackett, G. (1987). DRASTIC: a standardized system for evaluating groundwater pollution potential using hydrogeologic settings: U.S. environmental protection agency report 600/2-87/035, 622

Annor, A.E. and Olasehinde, P.I. (1996). Vegetation Niche as a remote sensor for subsurface aquifer. A geological study in Jere area, Central Nigeria. Journal of NAH, Vol. 7(1&2). 26 – 30

Babarinde, A. and Onyiaocha, G.O. (2016). Equilibrium sorption of divalent metal ions onto groundnut (Arachis hypogaea) shell: kinetic, isotherm and thermodynamics. Chemistry International, Vol. 2, 37 – 46

Civita, M. (1994). Vulnerability maps of aquifers subjected to pollution: theory and practice, Pitagora Editrice, Bologna (in Italian)

Doerfliger, N., Jeannin, P.Y. and Zwahlen, F. (1999). Water vulnerability assessment in karst environments: a new method of defining protection areas using a multi-attribute approach and GIS tools (EPIK method). Environmental Geology, Vol.39(2). 165 – 176

ESRI (1999). Getting to know ArcView GIS, 3rd edition, ESRI Press, California

Foster, S.S.D. (1988). Groundwater recharge and pollution vulnerability of British aquifers: a critical overview. Geological Society Special Publication, 130, London

Ibrahim, K.O., Gomo, M., Oke, S.A. and Yusuf, M.A. (2017). Vulnerability assessment of shallow aquifer hand-dug wells in rural parts of Northcentral Nigeria using AVI and GOD methods. The Pacific Journal of Science and Technology, Vol. 18(1), 325 – 333

Idowu, T.E., Nyadawa, M. and K'Orowe, M. (2016). Seawater intrusion vulnerability assessment of a coastal aquifer: North coast of Mombasa, Kenya as a case study. International Journal of Engineering Research and Application, Vol. 6(8), 37 – 45

Majolagbe, A.O., Adeyi, A.A. and Osinbanjo, O. (2016). Vulnerability assessment of groundwater pollution in the vicinity of an active dumpsite (Olosun), Lagos, Nigeria. Chemistry International, Vol. 2(4), 232 - 241

Mirzavand, M. and Ghazavi, R. (2015). A stochastic modelling technique for groundwater level frequency level forecasting in an arid environment using time series methods. Water Resources Management, Vol. 29, 1315 – 1328

NSDWQ (2017). Nigerian Standard for Drinking Water Quality. NIS:554, Nigerian, 1 – 14, Industrial Standard: Abuja, Nigeria

Obaje, N.G. and Abba, S.I. (1996). Potential for coal derived gaseous hydrocarbon in middle Benue trough of Nigeria. Journal of Petroleum Geology, Vol. 19, 77 - 94

Omotoso, O.A., Mamodu, M.O. and Ojo, O.J. (2011). Evaluation of geotechnical properties of laterite soils in Asa-Dam area, Ilorin, southwestern Nigeria. Journal of Applied Science and Technology, Vol. 3, 1-9

Recinos, N., Kallioras, A., Pliakas, F. and Schuth, C. (2004). Application of GALDITH index to assess the intrinsic vulnerability to sea water intrusion of coastal granular aquifers. Environmental Earth Sciences, Vol. 73(3), 107 – 1032

Sinreich, M., Cornaton, F. and Zwahlen, F. (2007). Evaluation of reactive transport parameters to assess specific vulnerability in karst systems', In: Witkowski, AJ, Kowalczyk, A, Vrba, J, Groundwater Vulnerability Assessment and Mapping, Selected Papers on Hydrogeology, Vol. 11, 21 – 32

Taylor, S.R. and Mclennan, S.M. (1995). The geochemical evolution of continental crust. Rev. Geophysics, Vol. 33(2), 241 – 265

Udoh, B.O. and Amadi, A.N. (2020). Evaluation of heavy metals pollution level in soils and plants around Ibeno Area, Akwa – Ibom State, Niger Delta, Nigeria. The Pacific Journal of Science and Technology, Vol. 21(1), 290 – 303

Van Stempvoort, D., Ewert, L. and Wassenaar, L. (1993). Aquifer vulnerability index: a GIS compatible method for groundwater vulnerability mapping. Canadian Water Resources Journal, Vol. 18, 25–37\

Vias, J.M. andreo, B., Perles, M.J. and Carrasco, F. (2005). A comparative study of four schemes for groundwater vulnerability mapping in a diffuse flow carbonate aquifer under Mediterranean climatic conditions. Environ Geol., Vol. 47(4), 586–595.

ISBN: 978-978-970-671-6

Proceedings of the 6th International Conference of the Nigerian Association for Engineering Geology and the Environment (NAEGE), Ibadan, Nigeria, 7th - 11th September, 2021 (Vol. 5), 2022.

Evaluation of Hydrocarbon Reservoir Characteristics and Volumetric Estimation Using Integrated Geophysical Methods in the "ZERO" Field, Niger Delta, Nigeria

Ugbor, C.C., Nwali, O.I. and Mamah, L.I.
Department of Geology, University of Nigeria, Nsukka, Nigeria.
***Corresponding E-mail*: osmondnwali6@gmail.com**

Abstract
Reservoir characterization using only conventional methods is subject to error due to some inherent uncertainties. Therefore, an integrated geophysical approach involving both structural seismic data interpretation attribute and rock physics analyses to characterize hydrocarbon reservoir and enable an understanding of the subsurface reservoir heterogeneity for optimal reserve estimation was investigated. 3D seismic volume and 5 well log data interpretations were undertaken with an emphasis on spatial litho-fluid distribution through rock attribute cross plots. Three horizons (R1, R2 and R3) mapped are laterally continuous across the field. Rock physical parameter cross plots of Gamma-ray (Gr) versus Poisson impedance (PI) analysis discriminate the target reservoir sand into four lithofacies as follows respectively for the Gr and PI: Sand zone: (0-75 (API) and 6000-16500 (ft./s*g/cc), Shale zone: 75-130 (API) and 16500-17800 ft./s*g/cc, Sandy shale zone: <75 API and >16500 ft./s*g/cc, and Shaly sand: >75 API and <16500 ft./s*g/cc. Two fluid types (oil and brine) were identified as areas of low acoustic impedance and Poisson impedance which signifies oil-filled sandstone, while the area of intermediate/high acoustic impedance and Poisson impedance signifies brine/shale. Three prospects (Geese, Larks and Cuckoos) were delineated from structural/quantitative interpretation. Formation evaluation showed high Net-to-gross, very good porosity, excellent permeability and low water saturation of 132.5 ft., 24.3 %, 2072.04 mD and 0.273 respectively. The estimated stock tank oil initially in place of the three identified prospects are 320, 51 and 19 million barrels (mbls) of oil, respectively.

***Keywords**: Correlation, Rockphysical Parameters, Seismic inversion, Formation Evaluation*

Introduction

The overriding aim of reservoir studies is to characterize and quantify the reserves. However, spatial reservoir heterogeneity has limited the successes of conventional reservoir characterization methods due to inherent uncertainties, which lead to inadequate results. The identification and classification of reservoir facies form part of the major challenges faced by the exploration geoscientist during field planning, appraisal and development drilling owing to the heterogeneous nature of the subsurface. Thus, the characterization of oil and gas reservoirs requires integrating different geophysical techniques for accurately building of reservoir models. The conventional approach to the identification and characterization of oil reservoirs involves the use of well-log data and seismic data. However, these approaches have its limitation as in the use of gamma-ray to discriminate between sand and shale in the presence of radioactive sands. Similarly, seismic data provide high-resolution images of the subsurface structure, but attempts to map fluids from seismic data may be misleading due to the ambiguity between lithology-fluid and lithology effects. Hence, technological advancements in seismic and borehole geophysics have made it easier to construct structural patterns, stratigraphic patterns and litho-facies variation of a reservoir with a high degree of consistency and accuracy through rock physics (petro-physical) analysis that strongly correlates with the lithology type (the reservoir lithofacies) and fluid content of a reservoir (Chen *et al*., 2012). Thus, through careful integration of the complementary information from these geophysical approaches, the limitations of each method can be overcome, and the strength of each exploited, that will be of help to fully understand the reservoir characteristics, improving the reservoir imaging and reducing uncertainties during field appraisal and development. Several authors including Anyiam*et al*. (2017), Bello *et al*. (2015) and Munyithya*et al*. (2019) have carried out reservoir studies using different geophysical analysis that cut across different aspects for interpreting the structures, stratigraphy and petrophysical properties of oil & gas fields in the Niger Delta. However, these studies either worked in isolation or followed a conventional approach. Therefore, this study seeks to integrate different geophysical approaches such as rock physics, cross-plot and seismic inversion analysis to reservoir evaluation for a comprehensive understanding of the structural configuration, spatial lithology distribution and fluid content distribution.

The Study Area

The study area (Fig. 1.) is situated in the coastal swamp Depobelt, the south-eastern.part of the Niger Delta sedimentary basin, within the apex of the Gulf of Guinea on the west coast of Africa, covering an area of about

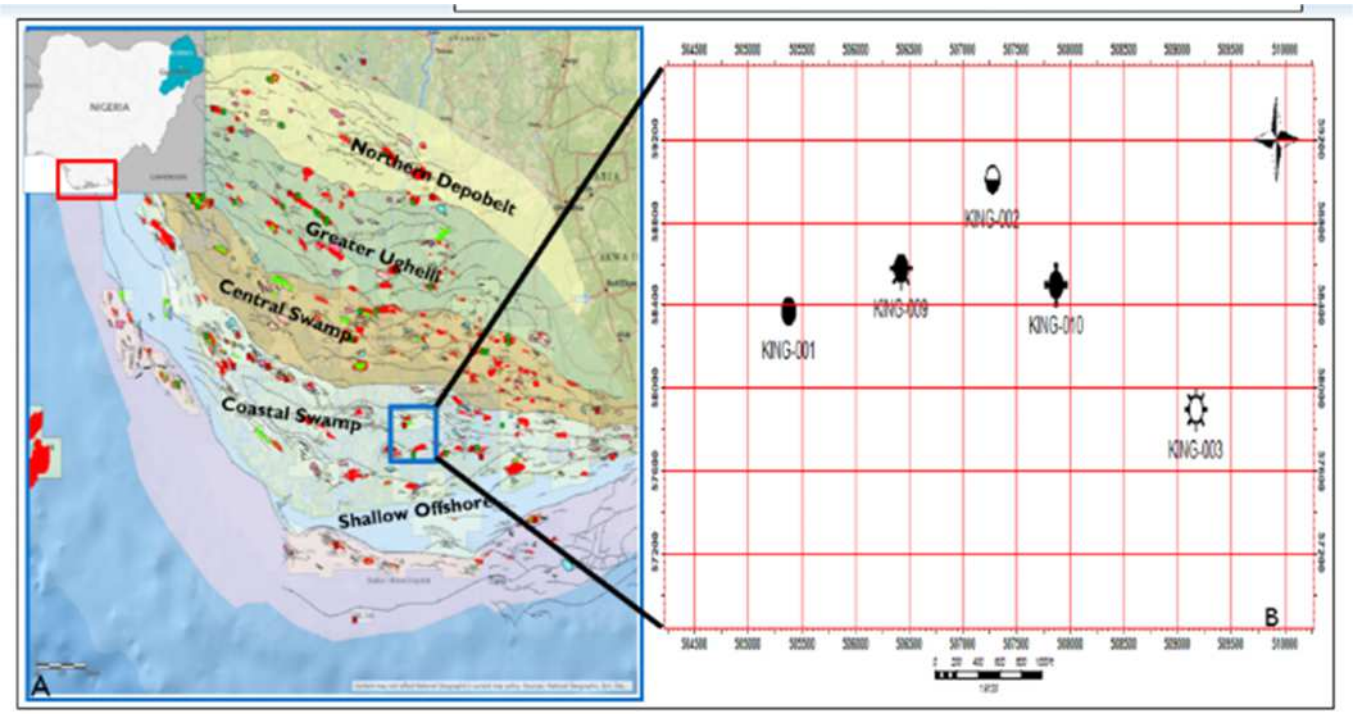

Fig. 1: (A) Map of Nigeria (inset) (modified after Doust and Omatsola 1990), showing the location of the Niger Delta, depobelts and the study area in the Central Swamp Depobelt; (B) Base map of the study area showing the positions of the studied wells

20000 km^2. Geologically the study area lies within the Niger Delta sedimentary basin, which evolved as a result of the Santonian-Early Campanian crustal deformation of Benue trough-a NE-SW folded rift basin that runs diagonally across Nigeria (Frankl and Cordry, 1967; Short and Stauble, 1967), formed simultaneously with the opening of the Gulf of Guinea and the Equatorial Atlantic in Aptian-Albian times, when the equatorial part of Africa and South America plate began to separate (Benkhelil, 1989), representing a failed arm of a rift triple junction. The Cenozoic Niger Delta consist of three major formations (Akata, Agbada and Benin) (Evamy et al., 1978), with one major existing petroleum system (Akata-Agbada) referred to as the tertiary Niger Delta petroleum system. The lithostratigraphic sequence ranges from the youngest Benin Formation, which is made up of alluvial and upper coastal plain sands (Avbovbo, 1978), predominantly continental fluvial deposits; the Agbada Formation, characterized by paralic interbedded sandstone and shale (Reijers, 1996) and the oldest Akata Formation, the primary source rock in the Niger Delta, consisting of uniform under-compacted shales, clays, and silts (Avbovbo1978) with its Basal unit characterized by dark grey shales, silts, and rare streaks of sand of probable turbidities flow origin (Doust and Omatsola, 1989) see fig. 2.

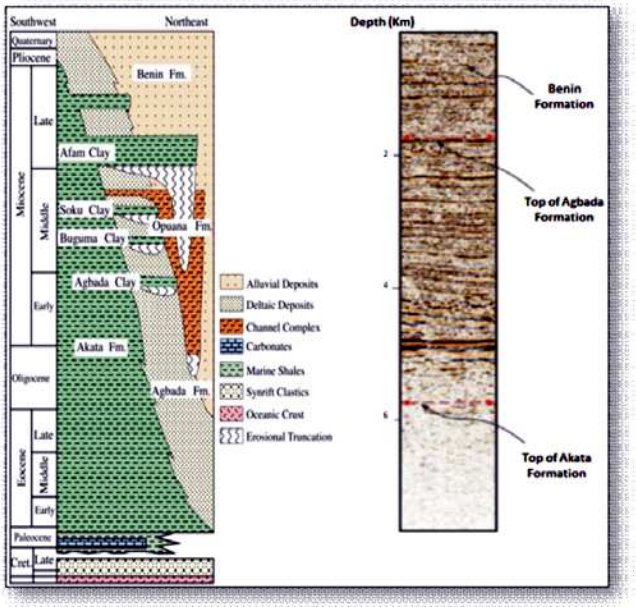

Fig. 2: Niger Delta regional stratigraphic configuration and variable density seismic display of the main stratigraphic units with corresponding reflector surface (Modified after Lawrence et al., 2002)

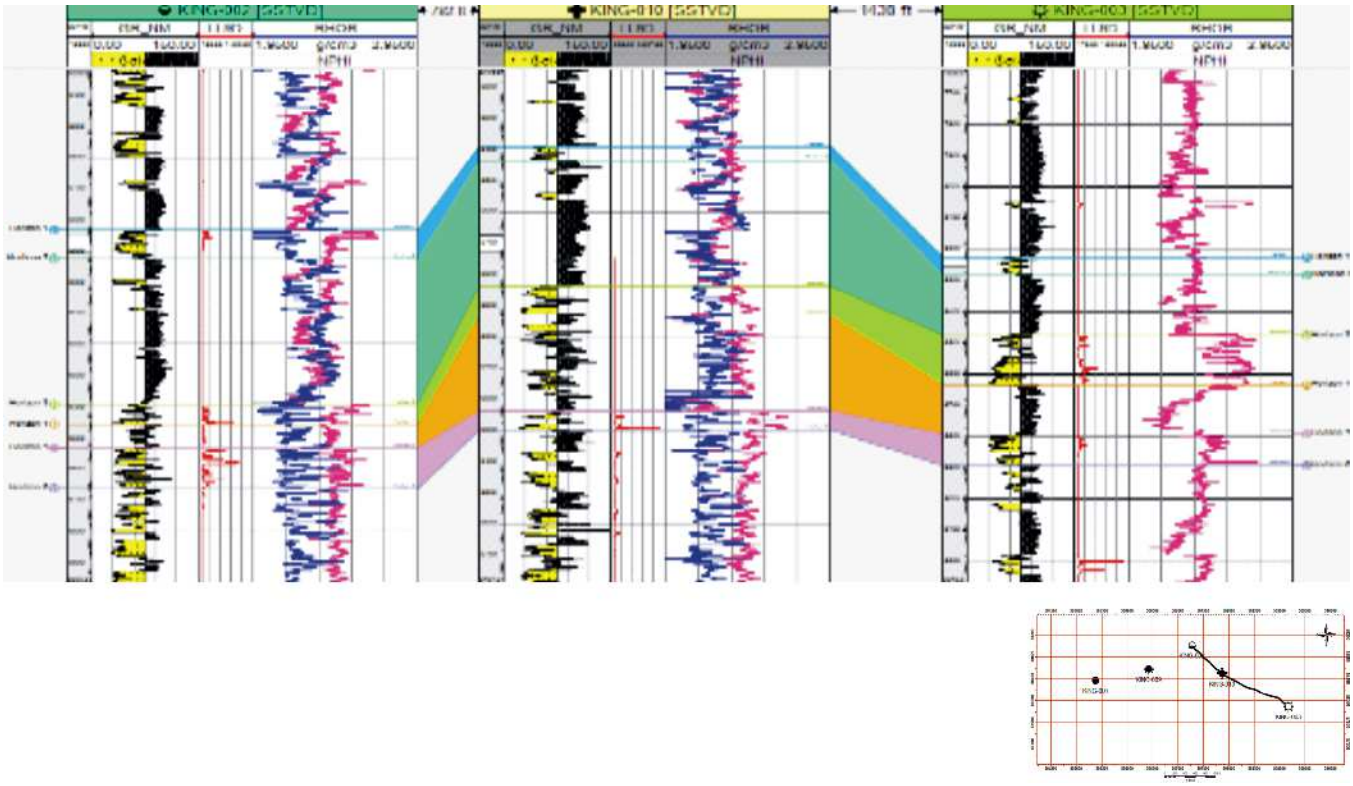

Fig. 3: The 3 reservoirs (R_1, R_2 and R_3) with R_1 as the target reservoir were correlated along dip direction across the selected three wells

Materials and Methods

The data set used for this study consist of five wells named KIN_001, KIN_002, KIN_003, KIN_009 and KIN_010 (Fig.1 and Table 1) with different logs (Gamma ray (GR), Resistivity (RT), Neutron (NPHI) Density (RHOB), Sonic (Δtp), Caliper and Porosity (Φ) logs) check shot data and post-stack 3D seismic data in Zgy format from "KINS Field onshore Niger Delta. This was prepared through a quality check and loaded into Petrel™ 2014 Interactive Petrophysics™ 3.4 and Hampson Russel ™10.3 relative to different geophysical analyses. Reservoirs were delineated along the depositional strike using gamma ray and resistivity log, forming the basis for petrophysical evaluation and a pointer to horizon mapping after seismic to tie well for structural and stratigraphic modelling of the field. The structural architecture of the study area was established via an overlay of fault picked and mapped horizon surfaces through time-to-depth conversion using a second-order polynomial equation given as TVDSS = -0.0007TWT^2 + 1.9703TWT - 647.01) derived from the check shot data. The interpreted horizons were imported into Hampson Russel software for quantitative seismic interpretation- involving rock physical parameter estimation, Cross plot analysis and post-stack model-based seismic inversion.

Table 1: Data availability table showing reference well and logs present in the wells.

WELL/LOG	KING_001	KING_002	KING_003	KING_009	KING_010
GR					
Resistivity					
Sonic					
Density					
Neutron					
Porosity					
Caliper					

Data
No Data

Results and Discussion

Reservoir Delineation & Well LogInterpretation

Three reservoirs (R_1, R_2 and R_3) with R_1 as the target reservoir were correlated along dip direction across the selected three wells (Fig.3). The reservoirs are laterally continuous. It occurred at the depth interval of 8835-9664(ft.), 8472-9243(ft.) and 8230-10230(ft.) for KING-002, KING-003 and KING-010, respectively along the well section window with an average thickness of 131.5, 58 and 138.2 ft for R_1, R_2 and R_3 respectively.

Seismic (Fault) Interpretation

The study area is structurally characterized by synthetic

(F1, F3, F4, F5, and F10) and antithetic (F2, F6, F8 and F9) faults. The interplay between these sets of faults (Listric faults) generated features like collapsed crests and back-to-back fault systems are consistent with the structural styles existing in the Niger Delta (Evamy et al., 1978) as shown in Fig. 4.

Seismic (Stratigraphic) Interpretation

The stratigraphic surface (horizon map) of the R_1 reservoir named H_D8500, relative to the approximate depth of occurrence, infers areas of structural high (anticline) at the northern part trending north-east and structural low (syncline) at the southwestern part of the map based on the contour values exhibiting three fault closure: One-way, two-way and three-way fault closure (Fig. 5a&b.) It was also observed, that seismic Attribute (root mean square and average energy) map shows the area of bright spot majorly occurring at the southwestern and north-easternpart of the field indicated with white ellipse (Fig. 6a&d) which is in conformity with the impedance slides map from model-based inversion.

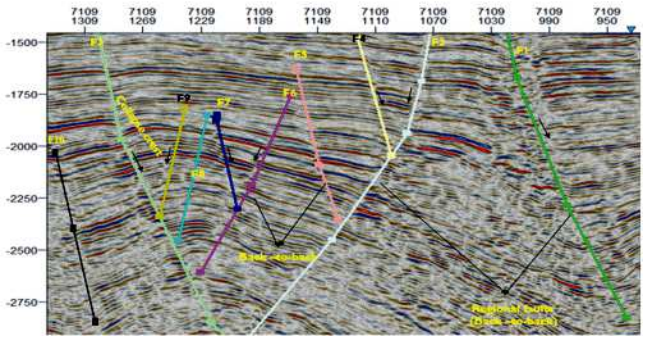

Fig. 4: Seismic section showing mapped faults and their interpretation

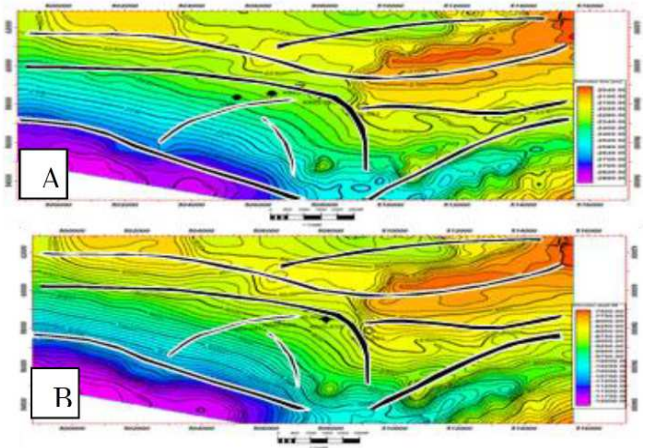

Fig. 5. Seismic surface attribute Map of horizon (H_D8500)showing (A) RMS Amplitude (B) Average energy. Encircled is the bright spot.

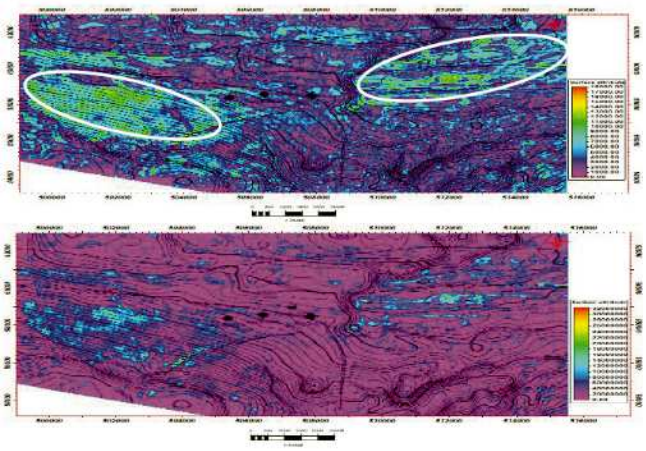

Fig. 6: (A) Time and (B) Depth structural map of the mapped horizon H_D8500 (R1_Top) showing a structural correlation in time

Rock Physics Analysis

Pseudo-log of the estimated rock physical parameters and measured petro-physical properties were presented in Fig. 7. There, sand is differentiated from shale, creating sand/ shale /sand sequence which serves as a guide in accurate reservoir delineation in the presence of radioactive sands.

Cross plot diagnostic interpretation.

For optimal characterization of the target horizon, the modelled elastic parameters and reservoir properties were cross-plotted for litho-facies and fluid content classification (Avseth, 2009; Chi and Han, 2009) using the most robust attributes. The most robust attributes identified are Poisson impedance versus gamma ray and Poisson impedance and water saturation due to their clear separation in rock physics template (RPT).

Cross Plot of Poisson Impedance Versus Gamma Ray

The results of Poisson impedance (PI) against Gamma ray (GR) colour coded with Poisson ratios show that area with low (PI), GR and Poisson ratio correspond to sand zone while area with high PI, GR and Poisson ratio corresponds to shale zone (Fig. 8). Sand zone has values between 0-75 (API is the unit of gamma-ray) and 6000-16500 (ft./s*g/cc) while area above 16500 (ft./s*g/cc) and below 75 API is described as sandy shale. Shale zone has range of values between 75-130API and 16500-17800 (ft./s*g/cc), while area below 16500 (ft./s*g/cc) and above 75 (API) is classified as shaly sand.

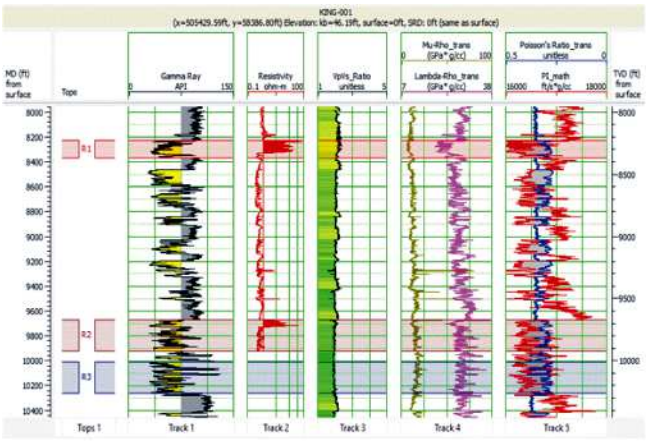

Fig. 7: Pseudo-log results (section) of measured and calculated elastic rock properties and delineated reservoirs at KING_010 showing well tops, gamma ray (track 1) Resistivity (track 2), Vp/Vs (track 3), lambda-Rho Muo-Rho (track 4) and PI, Poisson ratio (track 5)

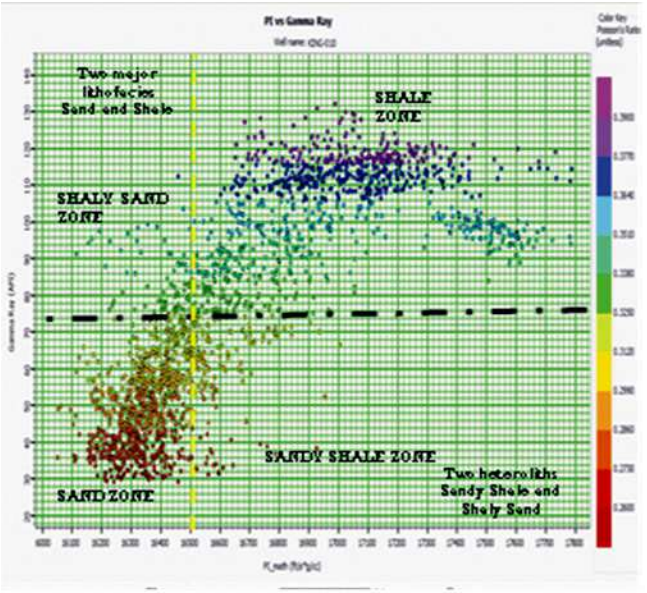

Fig. 8: Poisson impedance verses Gramma ray colour coded with Poisson ratio at H_D8500 delineating lithofacies classes

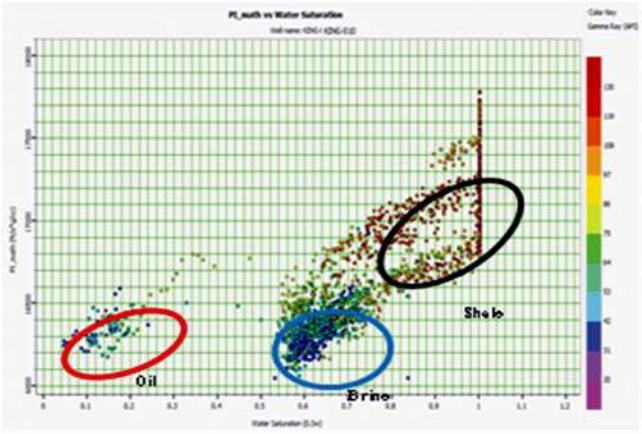

Fig. 9: Poisson impedance verses water saturation colour coded with grammar ray at H_D8500 showing pore fluid content

Cross Plot of Poisson Impedance Versus Water Saturation

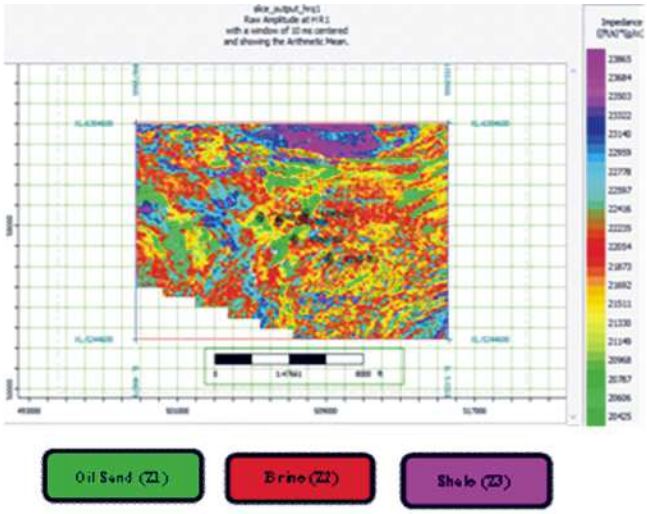

Fig.10: Horizon slice of acoustic impedance across reservoir one (H_D8500) showing low acoustic impedance as hydrocarbon filled sands, intermediate and high acoustic impedance as brine and shale

The cross plot of Poisson impedance and water saturation colour coded with Gamma-ray discriminates pore fluid content within a reservoir and their interrelation in defining a reservoir. This further clarifies the fluid content discrimination capacity of V_P/V_s Ratio versus P-Impedance of which its attribute is sensitive to both reservoir matrix and pore fluid. From the cross plots as in Fig. 9 shows that pay zone (red ellipse) has low PI, SW, and GR, shale (black ellipse)has high PI, SW and GR while (blue ellipse) having intermediate values represents the brine.

Formation Evaluation And Statistical Analysis

Table 2 shows the petrophysical characteristics of the target Reservoir (R_1) for the correlated wells.

Impedance Slice Analysis

Rock physics parameter analysis,a point data was extended into the whole field through post stack model-based seismic inversion analysis. Fig. 10 shows the rock attribute (acoustic impedance) derived from inversion analysis which was extracted from the impedance volume for the target reservoir centred at a 10ms time window (H_D8500-Reservoir one), confirms the inference of the cross plots and also within the target zone. Acoustic impedance values are from low to high and has a numerical range of 20425-23865(ft./s)*(g/cc). P-impedance was an effective rock

Table 2: Statistical analysis of log derived petrol-physical properties at well locations

Reservoir 1(H_D8500)										
Wells	Top(ft.)	Bottom(ft.)	Gross Thickness	Net thickness	N/G	Porosity(v/v)	SW	HS	V_Sh	Permeability (mD)
king_002	9203.5	9368	164.5	163	0.991	0.246	0.556	0.444	0.185	2099.80
king_009	8935.5	9079.5	144	141.75	0.984	0.23	0.779	0.221	0.162	1965.23
king_010	8886	8975	89	89	1	0.252	0.755	0.245	0.101	2151.01
Average			132.5	131.25	0.992	0.243	0.610	0.303	0.149	2072.04

attribute that fairly discriminated oil sand from brine sand. It indicated a gross thickness value range of 89-164.5 ft. with an average value of 132 ft. The porosity ranges from 23 to 25%, and an average value of 24% which is a very good porosity for oil-producing sandstone reservoirs and permeability values between 1965.23-2151.01 millidarcys (mD) with an average of 2072.04 showing an excellent permeability.

Prospect Delineation and Volume Estimation

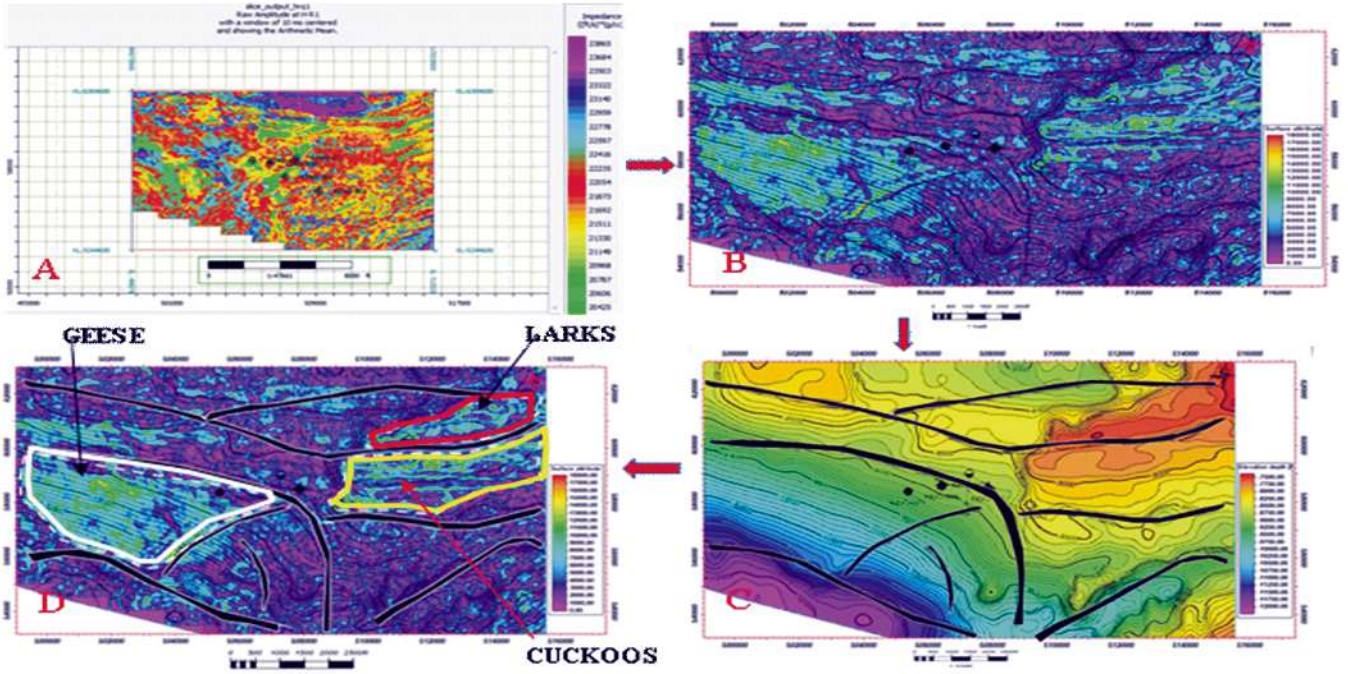

Fig. 11: Prospect identification showing integration of; (A) Acoustic impedance map-Fluid identification (B) RMS amplitude-Direct hydrocarbon indicator and area of payable zone (C) Depth structural map- structural configuration/trapping mechanism (D) Prospect identified- Named Geese, Larks and Cuckoos.

The area on the reservoir horizon map that are hydrocarbon-bearing was delineated using the integration of an acoustic impedance slice map, seismic amplitude map and depth structural map as shown in Fig. 11 (a-d). In conjunction with the thickness of the reservoir and other petrophysical parameters. The Stock Tank Oil Initially In Place (STOIIP) was estimated using eq. 1. (Table 3).

Table 3: Results of Oil Volume Estimates for delineated prospects at H_D8500

Reservoir properties Prospect	Gross rock volume (Ft3)	Net to gross (AV.N/G)	Porosity (av.phi)	Hydrocarbon saturation (av.sh)	Formation volume factor (fvf)	Stoiip (stb)	STOIIP (Mbls)
GEESE	**25,334,808.171**	**0.992**	**0.243**	**0.727**	**1.35**	**3,288,790.493**	**329**
LARKS	**3,916,102.409.41**	**0.992**	**0.243**	**0.727**	**1.35**	**508,361.472**	**51**
CUCKOOS	**1,484,075.185**	**0.992**	**0.243**	**0.727**	**1.35**	**192,652.430**	**19**

$$STOIIP = \frac{GRV*N/G*\phi*Sh}{FVF} \quad \text{.....(1)}$$

where STOIIP= stock tank oil initially in place, GRV = Gross Rock Volume (Area of the prospect x thickness of the prospect),

N/G = Net –to – Gross, ϕ = Porosity, Sh = Hydrocarbon Saturation, and FVF = Formation Volume factor (see Table 3).

Conclusion

Integrated geophysical analysis studies in Zero field provided a robust interplay that enhanced the characterization of the reservoir identified in the field. Results from well log correlation and formation evaluation identified three reservoirs (R_1, R_2 and R_3) which are laterally continuous across the study field. The horizon surfaces corresponding to R_1, named: H_D8500, revealed that the study field is structurally high (anticline) and low (syncline) at the north-eastern and southwestern part of the field and two faulting system exist in the field which includes regional and listric (antithetic and synthetic) fault system supporting the entrapment of hydrocarbon.Cross plot analysis classifies the reservoir into two mainlithofacies (sand and shale) and two heteroliths (sandy shale and shaly sand). The sand lithofacies has low PI of <16500 (ft./s*g/cc) and low gamma ray of <75 API while shale lithofacies has high PI and gamma ray of > 16500 (ft./s*g/cc) and > 75 API. Poisson impedance analysis classified reservoir pore fluid into oil and brine.

The oil-bearing reservoirs have low Poisson impedance, while water-bearing one has an intermediate value of Poisson impedance. The petrophysical parameters evaluation shows that the target horizons have very good porosity and excellent permeability values of 24% and 2072.04 milli Darcy (mD) respectively, with high net-togross thickness and low water saturation of 132.5 ft. and 0.273 respectively. The estimated stock tank oil initially in place of the three identified prospects (Geese, Larks and Cuckoos) through the grid method are 320, 51 and 19 million barrels (mbls) of oil, respectively, giving a total of 390 mbls of oil.

References

Anyiam, O. A., Maduewesi. C. O., Ibemesi P. O. &Okwara. C. O. (2017): Reservoir quality studiesand prospectidentification of a field in coastalswamp depobelt. Petroleum and Coal, 59(4): pp. 505-515.

Avbovbo,_A._(1978). Tertiary lithostrati-graphy of Niger Delta. American Association of Petroleum Geologists Bulletin, 62: pp. 96-200.

Bello, R. I., Linda, C.C. &Onifade, Y.S. (2015). Cross plotting of rock properties for fluid and lithology discrimination using well data in aNiger delta oil field. Journal of Applied Science, Environment and Management, 19(3): pp. 539-546.

Benkhelil, J. (1989): Yhe evolution of the Cretaceous Benue Trough, Nigeria. Journal of African Earth Sciences 8, pp. 251–282.

Chen, J., and G. M. Hoversten (2012): Joint inversion of marine seismic AVA and CSEM data using statistical rock physics and Markov random fields. Geophysics, 77(01), pp. R65– R80,

Chi, X., Han, D., 2009: Lithology and fluid differentiation using rock physics templates. The Leading Edge 28(1) DOI: 10.1190/1.30664147.

Doust, H. and Omatsola, E., (1990): Niger Delta: In Edwards, J. D. & Santogrossi, P.A. (Eds.), Divergent/passive margin basins: American Association of Petroleum Geologists Memoir, 48: pp. 239-248.

Evamy, B.D., Haremboure, J., Kamerling, P., Knaap, W.A., Molloy, F.A. and Rowlands, P.H., (1978): Hydrocarbon habitat of Tertiary Niger Delta. American Association of Petroleum Geologists Bulletin, 62: pp. 1-39.

Frankl, E.J., & Cordy, E.A. (1967): The Niger Delta oil province: Recent developments onshoreand offshore. Seventh world petroleum congress proceedings, Mexico, 2: pp. 195-209.

Munyithya, J. M., Ehirim, C. N., &Dagogo, T. (2019): Analytical evaluation of rock attributes for hydrocarbonreservoir charac-terization in an eastern Niger delta onshore X field, pp. 50- 59.

Reijers, T.J.A., Petters, S.W. &Nwajide, C.S. (1997): The Niger Delta basin. In: Selley, R. C. (Ed), African basins, Amsterdam, Elsivier science, sedimentary basins of the world, 3: pp. 151–172.

ISBN: 978-978-970-671-6

Proceedings of the 6th International Conference of the Nigerian Association for Engineering Geology and the Environment (NAEGE), Ibadan, Nigeria, 7th - 11th September, 2021 (Vol. 5), 2022.

The Impacts of Soil Erosion on Buildings in Parts of Minna Sheet 164, North-Central Nigeria

Sidi, A.A.[1], Yisa, A.M.[1] and Liman, H.M.[2]

[1]Faculty of Applied Sciences and Technology, Department of Geology and Mining, Ibrahim Badamasi Babangida University, Lapai, Nigeria.

[2]Faculty of Natural Sciences, Department of Geography, Ibrahim Badamasi Babangida University, Lapai, Nigeria.

Corresponding E-mail: **aasidi@ibbu.edu.ng**

Abstract

Field geologic mapping and assessment of the impact of soil erosion on buildings were carried out in parts of Minna, sheet 164 SW North-central Nigeria. The rocks in the area are Granite and Granite-Gneiss with medium to coarse grained textures, primarily trending in the NNW-SSE. The exposed rocks in the vicinity also showed a high rate of weathering. The level of erosion activities on nearby structures, including bridges, was revealed by the stream channel mapping. The effects were especially noticeable in areas where structures were placed randomly in the catchment areas of the streams. Loose soils and waste dumping in the stream channels which block the waterways are the contributing factors in the rate of soil erosion around the localities, especially during the rainy seasons. To control the rate of this hazard on the buildings, the households within these areas have resulted in the use of car tyres as a means of controlling the loss of soil to erosion; in addition to reinforced concrete structures to stabilize the soils and control the soil erosion. It is recommended that adequate awareness of the safe protection of the drainages should be conducted to reduce the damages that may result from this geologic hazard.

Keywords*: Geological Mapping, Geologic Hazards, Soil Erosion, North-Central, Nigeria*

Introduction

The damage done to buildings all over the country as a result of soil erosion was always in the news emanating from both the broadcast and the print media in the past few years and the situation is becoming too worrisome that urgent measures or actions need to be taken to control the menace.

Niger State is one of the states often badly affected by the damages to or destruction of buildings resulting from soil erosion. The study area is situated in the lower part of Minna on the bases of elevation and stream flow direction and therefore prone to annual heavy seasonal running surface water erosion especially during rainfall periods. This running surface water often overflow the boundaries of the streams, wash away the soil and cause damages to buildings or perhaps destroy completely some buildings along and within close proximity to the streams. The damages done to the buildings by soil erosion always involve loss of human lives especially in situations when such disasters happened in the night times.

Soil according to (Zaman *et al,* 2018) is defined as the top layer of the earth's surface that is capable of sustaining life. Soil erosion is the wearing way of a field top soil by the natural physical force of water and wind (Balasubramanian, 2017).

Soil erosion is a naturally occurring process that affects all land forms. It is a global issue and it has been in the news over the years due to the damage it has done to land, property, infrastructures and even loss of human lives in several countries (Balasubramanian, 2017). Telkar *et al.* (2018) are of the opinion that soil erosion may be a slow process that continues relatively unnoticed or it may occur at an alarming rate causing serious loss of top soil. Soil erosion reduces land for buildings purpose and contributes to the pollution of adjacent water courses, wet lands and lakes (Balasubramanian, 2017).

The Study Area

The study area is part of Minna Sheet 164 SW North-Central Nigeria (Fig. 1) It is located within latitude ($09^0$34'N and $09^0$38'N) and longitude ($006^0$30'E and $006^0$34'E). The area is accessible through the major roads from western bye-pass road linking Kpakungu round about a commercial area. It can also be accessible from the east through buildings material bye-pass road. The geomorphology of the area is characterized with rugged topography with outcrops of granitic rocks surrounding the area.

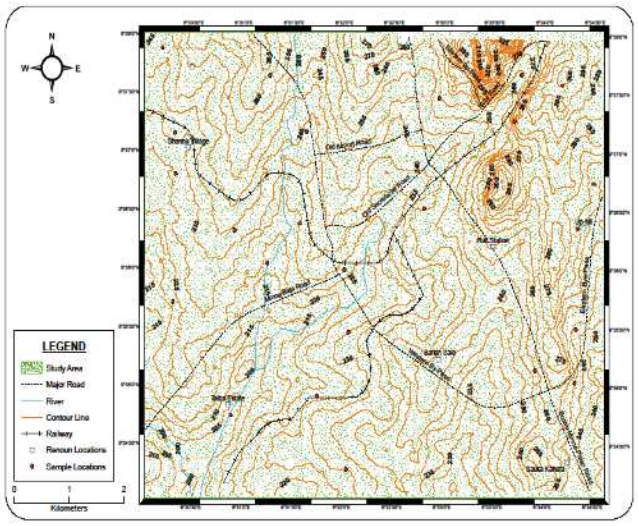

Fig. 1: Topographical map of the study area (modified after OSGOF, 2021)

Materials and Method

Reconnaissance Survey

The primary data in respect of the study area were collected through reconnaissance. The visits were made to the areas to determine the extent of the study area, observe the nature of outcrops in the area in addition to the information obtained from the topographical map covering the same area. Further observations were made on the nature and conditions of the access roads within the areas bearing in mind that the conditions of access roads certainly play significant roles in erosion issues.

Field Geological Mapping

The mapping was systematically carried out by taking traverses along man made infrastructures, foot paths, roads and natural features. Twenty nine locations were mapped and the latitude and longitude of these locations were recorded using the Global Positioning System (GPS) and compass clinometers was used to measure the strike direction of joints and dip angles of the rocks, while measuring tape was used to measure the width and length of veins. Hand lens was used to identify the color, mineralogy and grain size of the rocks, geological hammer was used for sampling of the rocks. The mapping and the physical field observation of the area was carried out to establish the existence of the features contributing to or likely to contribute to soil erosion for example, presence of permanent or seasonal streams, natural and artificial drainages, type of soil erosion and vegetation's, etc.

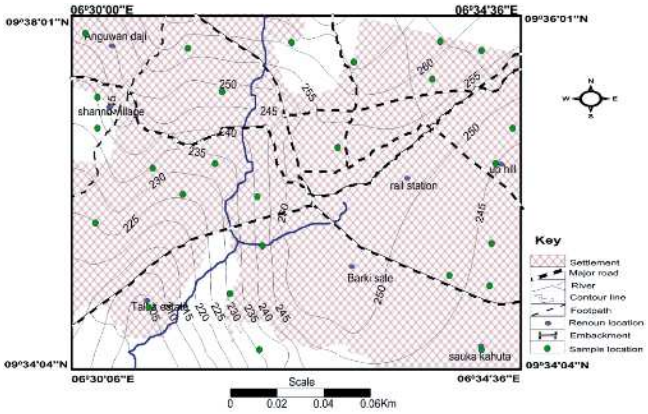

Fig. 2: Fact map of the study area with sample locations

Results

Results of geological field mapping conducted are presented in figure 2 and 3 and the rosset diagram of structural trends of the rocks is presented in figure 4.

The rock types in the study area are mainly Granite and Granite-Gneiss. The predominant rock type is the Granite with principal structural trends of NNW (Fig.4) and some minor trends occurring in different directions. Majority of the Granites have higher elevations than the Granite-Gneiss which suggests the susceptibility of the Granite-Gneiss to weathering activities. Macroscopic description of the rock samples revealed the Granites are mainly composed of biotite and few quartz and feldspar with medium to coarse grain textures. The structural deformations observed in the outcrops were fracture, faults, Joints, exfoliation and quartz vein intrusions. Different weathering activities have acted on the rocks subjecting them to weakness and subsequently erosion. Pegmatitic intrusions were also observed in most of the rock suggesting they may be mineralized.

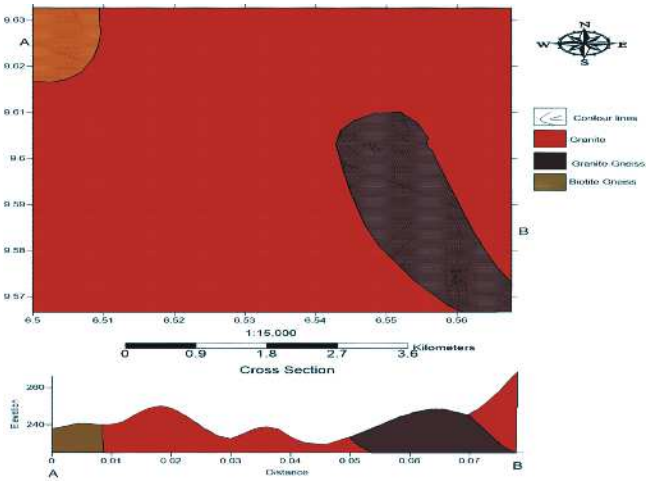

Fig. 3: Geological map of the area

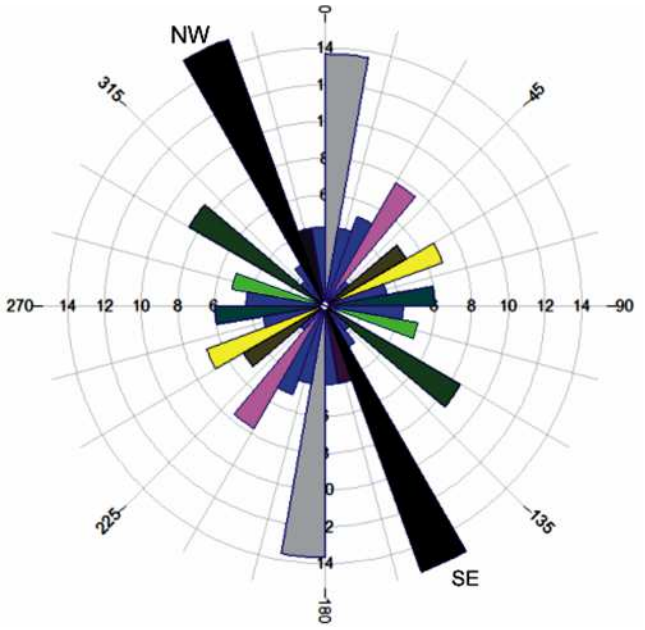

Fig. 4: Rosset Diagram with principal joint direction NNW

The encountered geological structures in field are mainly Joints, fractures, ex-foliation and intrusions. These are important in the understanding of the geological history of the area and can also help in evaluating their significance for engineering hydro and economic geology.

The joints observed in the field were mostly non-continuous as they occurred only at the surface. Some of them formed joint system and can be recognized. The Joints may possibly have resulted from orogenic events and serves as conduit from which groundwater can get penetrated to form groundwater reservoirs. The joints could pose some challenges and need to be avoided for engineering geologic structures even though they are not large scale joints. Plate 1 show a typical joint observed in the study area.

Faults observed in field were not of large scale. Most of them have their planes clearly defined. The faults were by forces acting against each other creating an oppositional movement and causing the rocks to crack and then blocks shifted.

The quartz intrusion observed were milky colour in appearance and may contain some valuable minerals like gold. Few of them were large scale intrusions and thick while some were small scale intrusions but elongated and thin. The small scale quartz veins were discontinuous and whitish in colour. The pegmatite intrusions observed in the field were not large. Some of them intruded the rocks at the middle, from the side and few from the bottom. Muscovite mica was observed in most of them. Plate 2 is typical quartz vein intrusion recorded in one of the locations visited.

Plate 1: Set of Joint observed in Shanu Village (09^0 37' 44" N, 006^0 30' 16" E)

Plate 2: Quartz vein observed in Sauka Kauta (09^0 34' 37" N, 006^0 32' 29" E)

Soil Erosion

The impact of soil erosion on the sides of the major stream is also being felt by the residents of the nearby buildings to the extent that the occupants of the building on the bank of the stream mapped have to use old tyres (plate 4) and other local materials to prevent the erosion from extending to their buildings. It was also intended that the damaged of soil erosion from the east is not only being eroded deeper down the basement, but also widening both sides of the channel, thus causing serious damages to a road within the vicinity. The type of flow within this area is known as turbulent from which the water at the meander of the channel cause over flowing to other areas within the catchment.

It can be observed that two erosion channels from east and west flows in to a major stream respectively and all the three streams have been affected by soil erosion since none of them is controlled. While erosion has washed away the drainage of stream from east up to some meters down to the Basement, the effect of soil erosion from west is worse as the depth of the drainage is about 2.7 meters from the datum level. The affected portions of erosion channel from west are however being reclaimed (refilled) by using same as refuge dump (plate 3)..

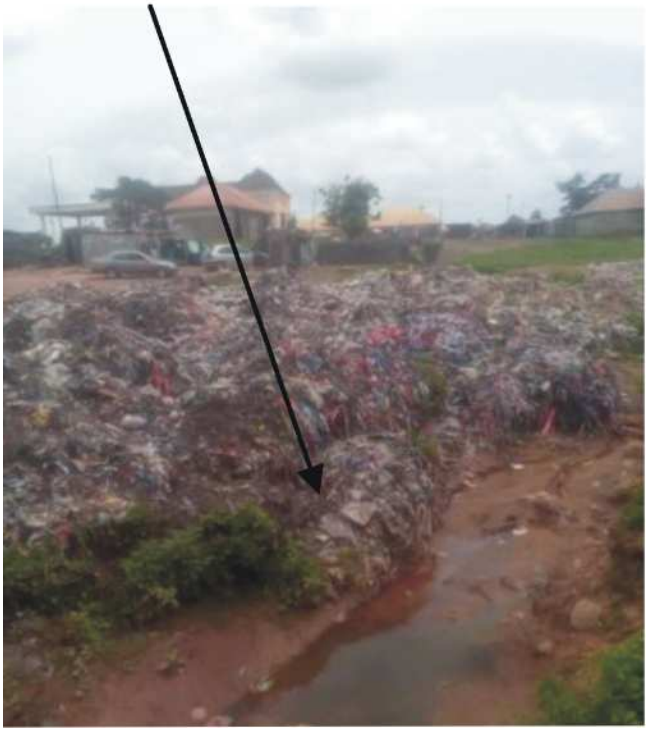

Plate 3: Refuse was used to reclaim some affected place (09^0 35' 40" N, 006^0 31' 13" E)

Plate 4: Tyres were used to stop soil erosion at Kpankungu (09^0 35' 44" N, 006^0 31' 25" E).

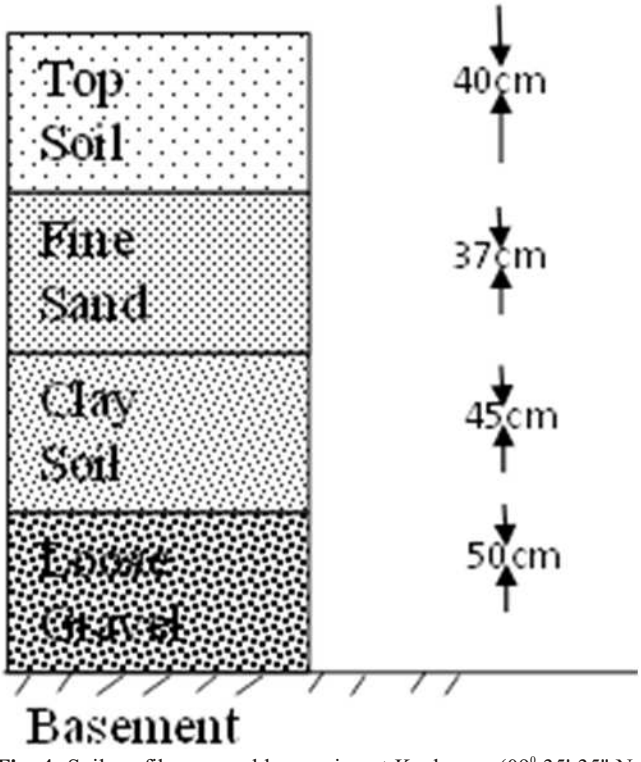

Fig. 4: Soil profile exposed by erosion at Kpakungu (09^0 35' 35" N, 006^0 31' 16" E)

The observed drainage channel badly affected by soil erosion along Kurmi Moses Kagara Street (plate 5), Tunga South Western Minna give account of the erosion devastation in that location. Some portions of the drainage channels with less resistance soil structures

with V Shaped are formed in the rocky portions of the channels. The rocky nature of these portions prevents the running water from washing off such areas but negatively aid the running water to overflow the drainage channel boundaries to destroy nearby building structures constructed on less erosion resistances soil basements.

Plate 5: V-shape resistant soil structure formed in the rocky portions of the drainage channels in Tunga (9^0 34'20"N, 6^0 33' 19" E)

Plate 6: (left), one side drainage was cast to prevent soil erosion in Sauka (9^0 35'28"N, 6^0 31' 18" E)
Plate 7: (right), building partially affected by soil erosion in Tunga (9^0 34'24"N, 6^0 33' 1" E)

At Barkin Sale area, serious washed off by erosion due to the absence of drainage channel along its sides were observed. A random measurement taken with a tape indicates that erosion has washed away almost a meter of the average level of the road and make most of the houses along the road inaccessible by motor vehicles and motor cycles plate 9, efforts by communities to control erosion has yielded some results (plate 10).

Plate 8: Building destroyed by soil erosion in Tunga (9^0 34'29"N, 6^0 34' 1" E)

Plate 9: (left) wash away access road by erosion at Barkin Sale area (9^0 35'8"N, 6^0 31'29" E)
Plate 10: (right) Stones was used to prevent further washing away of soil erosion in Barkin Sale (9^0 35'8"N, 6^0 31'29"E)

Conclusion

Observations from the area of study indicate that three sites have been affected by major soil erosions. The residents of these areas have turned the drainages in to refuse dumping sites. The available treas which can also contribute to the firmness and stability of the soil within the study area are sparely distributed this make erosion impact on soil greatest at those locations. Government agencies responsible for the control and management of erosions should be adequately empowers to take responsible decisions for the benefits of all.

References

Balasubramanian, A. 2017: Methods of Controlling soil Erosion. University of Mysore 365-496

Ofomata, G.E.K. 1985: Soil erosion in Nigeria: the views of a Geomorphologist. *University of Nigeria Inaugural Lecture Series* No.7. Nigeria.

Olubunmi, F.E. and Olorunsola, O.E., (2010): Evaluation of the Status of Heavy Metal Pollution of Sediment of Agbabu Bitumen Deposit Area, Nigeria. *European Journal of Scientific Research,* 41, 373-382.

Telkar, S. N. Pote S., 2018: Soil erosion types and their Mechanism. Biomolecule Reports

Umaru, E. T., Lami. M. H., 2018: Impact of gully erosion on Land use/Land Cover in Bida Town Niger State, Nigeria. *International Journal of Geography and Environmental Management* Vol.4 No 2.

Zaman, U. M., Bhat S., and Sharma A 2018: Methods to control soil erosion. International Journal of Pure & Applied 3(5).

ISBN: 978-978-970-671-6

Proceedings of the 6th International Conference of the Nigerian Association for Engineering Geology and the Environment (NAEGE), Ibadan, Nigeria, 7th - 11th September, 2021 (Vol. 5), 2022.

Rapid Estimation of Soil Engineering Properties Using Mid-Infrared Spectroscopy and Partial Least Square Regression

Fakeye, A.M.[1] and Ige, O.O.[2]

[1]Road Research Department, Nigerian Building and Road Research Institute;
[2]Department of Geology and Mineral Sciences, University of Ilorin, Ilorin, Nigeria
Corresponding E-mail: **afakeyespice@gmail.com**

Abstract
Assessment of soil propertiesis crucial in many engineering projects and conventional methods of determining them are expensive, tedious, time-consuming and invasive. This study examines the potential of soil mid-infrared (MIR) spectroscopy to rapidly estimate the key engineering soil properties. Fifty selected air-dried soil samples from different Basement Complex rock of Southwestern Nigeria were subjected to Fourier-Transform-Infrared-Spectrometric (FTIR) analysis within the MIR region (4000 – 400 cm^{-1}) of electromagnetic radiation. Optimal set of spectra were selected in attempt to remove non-informative bands, reduce complexity of calibration model and increase predictive ability of soil spectra. Soil properties like percent sand and clay, liquid limit, plasticity index, optimum moisture content, maximum dry density and soaked California Bearing Ratio were obtained from reference data and calibrated to Savitzky-Golay (SG) first derivative MIR spectra using partial least square regression (PLSR) method. The result shows that coefficient of determination (R^2>0.6) was obtained for full cross-validation, with root mean square error of 4.32 and ratio of performance to the derivative (RPD = 2.1) for soil properties. The results suggested that MIR-PLSR has potential to rapidly estimate key soil engineering properties. Further worksare recommended with focus on using diverse non-parametric data mining techniques to rapidly estimate soil characteristics.

Keywords*: Mid-Infrared Spectroscopy, Clay minerals, Coefficient of Determination, Ratio of Performance Derivative, PLSR, Savitzky-Golay Derivative*

Introduction

There is an increasing demand for comprehensive information on engineering properties of soils which are often obtained through complex conventional methods. The most essential parameters in geotechnical engineering are the soil moisture content, plasticity index, cohesion, unit weight, grain size distribution, porosity, etc. These properties are important in determining bearing capacity and slope stability of soil. However, they are tedious, relatively expensive, time-consuming and require experienced skilled operators with large amount of soil materials as specimen. Several tests have been used to provide rapid indicators of soil functional capacity for preliminary engineering investigations. These include particle size analysis, consistency limits, linear shrinkage, moisture content, density, California Bearing Ratio (CBR), etc. Consistency limits are reported to correlate well with shear strength, compressibility and permeability (Sridharan, 2014). Because conventional methods are not only expensive, slow and invasive (Mousavi et al., 2021), but involve physical destruction of the entire soil system, a quick and acceptable method is needed for rapid estimation of soil properties.

Since early 2000, reflectance spectroscopy has been introduced as a quick method to estimate various soil properties. Most of these works (Brown et al., 2006; Tian et al., 2013; Mousavi et al., 2019, 2021) reveal a good correlation between the index properties of soil and reflectance spectroscopy. This method is quick, simple, timely, non-destructive and less expensive than the conventional methods. In soil engineering, many studies have been conducted on the applications of spectroscopy for estimating soil engineering properties, such as clay content, Atterberg limits, swelling potential, CBR, unconfined compressive strength (Sorensen and Dalsgard, 2008; Mousavi et al., 2019, 2021; Yitagesu et al., 2009; Waruru et al., 2014). These studies have shown that spectroscopy combined with partial least squares regression (PLSR) can serve as a fast technique to estimate soil engineering properties with acceptable results. Many researchers have recognized PLSR as the most common method for estimating engineering properties of soils (Goetz et al., 2001; Waruru et al., 2014; Yitagesu et al., 2009). Mousavi et al. (2019) used PLS combined with backpropagation of neural network (PLS-BPNN) to construct empirical prediction models for estimating Atterberg limits and unconfined compressive strength (UCS) from their respective reflectance spectra and their results indicated a high potential for spectroscopy. Tian et al. (2013) carried out two-band combinations of spectra in soil indices (difference index and ratio index) in linear and non-linear regression analyses in order to

estimate soil organic content. Their results showed high performance of PLS and PLS-BPNN with higher prediction accuracy.

One major limitation of soil spectroscopy is the fact that soil spectra are non-specific, weak and broad due to overlapping absorptions of soil constituents, often available at small concentrations in the soil (Rossel and Behrens, 2010). However, the variations in the physical and mechanical properties of soil which are associated with the functional groups in the electromagnetic region create detectable spectral features via reflectance spectroscopy (Aichi et al., 2009, Conforti et al., 2015). In general, the reflected energy of the soil depends on the organic and mineral compounds, soil moisture content, and optical-geometric scattering due to surface roughness. Some earlier researchers applied PLSR analysis for estimating soil properties in the visible – near infrared (Waruru et al., 2014) and shortwave infrared (Kariuki et al., 2003) regions. Few studies tested the capability of mid infrared spectra in estimating engineering properties. Therefore, the objectives of the study were to determine the potential of mid infrared spectroscopy as a quick inexpensive tool in estimating soil properties and compare the accuracy of the model after correcting the baseline changes.

Materials and Methods

Study Area and soil sampling

A total of fifty soil samples were collected from 10m distance away from the corridor of Ilorin - Kabba highway. The highway overlies the Basement complex of Southwestern Nigeria covering approximately 15,612km^2 and bounded by latitude 7°25'N - 8°40'N and longitude 4°30'E – 6°45'E (Fig. 1), with a low to moderately high elevation ranging from 200 to 800 m above mean sea level. Temperature of the area ranges from 25° – 35°C with a mean annual rainfall of 1200mm. Due to heavy rainfall, considerable moisture change occur in the soils which dries up at prolonged dry season.

The soil collected from the study area were developed over three lithologic units: the migmatite - gneiss complex (32 samples), the meta-sediments (11 samples), and the older granite series (7 samples), but predominantly migmatite – gneiss composed of migmatite and banded gneiss. Others are flaggy quartzite with biotite gneiss, undifferentiated schists, porphyritic granite (porphyroblastic), and medium to coarse-grained biotite and hornblende granite. Strategic soil sampling collection followed a 3 by 5km interval distance (Fig. 2) at a depth of 0.8 – 1.5m overlying the geologic units within the area. Prior to laboratory analyses, the soil samples were air-dried at 30 – 35°C for two week where the soils were well dried and gently sieved with 2mm sieve.

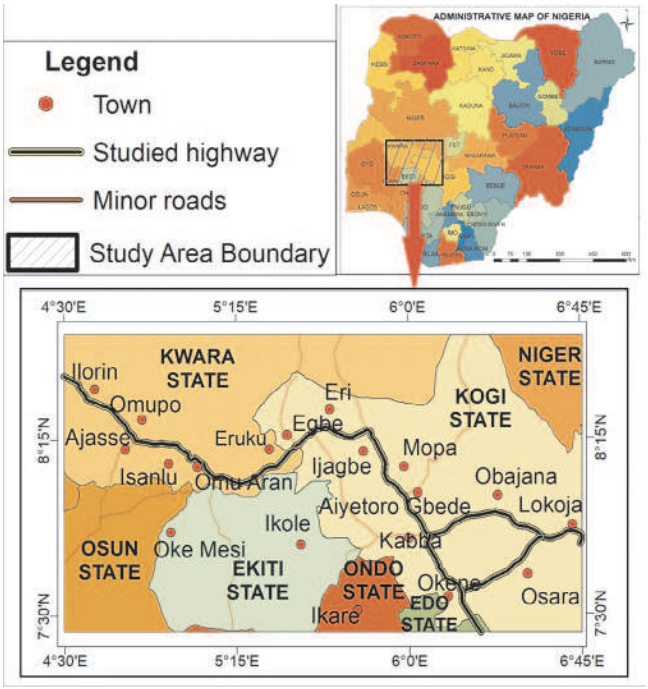

Fig. 1: Map of the study area (inset: map of Nigeria)

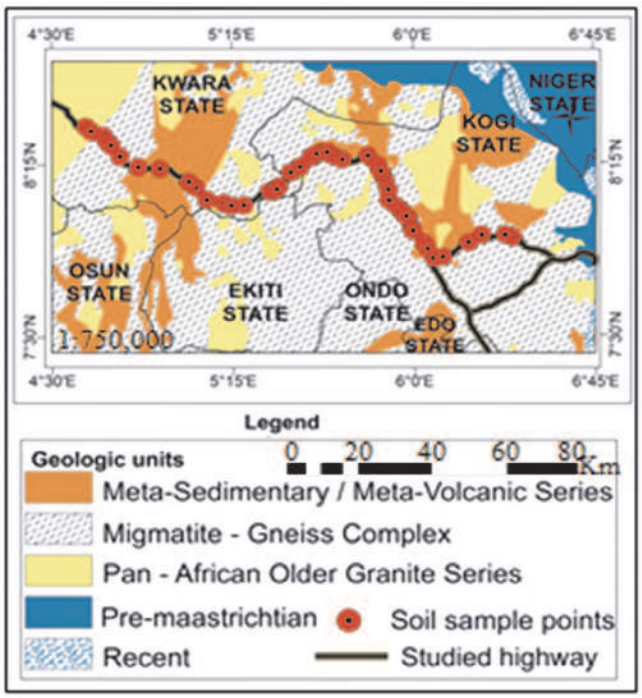

Fig. 2: Sample location and distribution of geological units underlying study area (Source: NGSA, 2004).

Laboratory geotechnical soil properties

Geotechnical analyses of soil were conducted based on BS 1377: 1990 standard method. The index properties include particle size distribution by sieve (gravel and sand) and hydrometer (silt and clay) methods, moisture content, liquid limit (LL), plastic limit (PL) and plasticity index (PI) which is the numerical difference between LL and PL. Other properties such as optimum moisture content (OMC), maximum dry density (MDD) and California Bearing Ratio (CBR) were also determined following the BS 1377 (British Standard 1990). The compaction was achieved using modified Standard Proctor method. Soil activity was determined based on Skempton (1953) as the ratio of plasticity index and percentage of clay. The soil was classified in accordance with the Unified Soil Classification System (USCS).

FTIR measurements and spectra preprocessing

About 10mg of each soil sample was pulverized to 0.07mm size (at 105°C) and carefully subjected to spectral measurement under laboratory conditions using a Bruker Vertex 70 Fourier Transform Infrared Reflectance spectrophotometer of spectral resolution between 2 – 4cm^{-1} with an accuracy of ±4 cm^{-1} and spectral range in the MIR region (4000cm^{-1} – 400cm^{-1}) with a resolution of 2cm^{-1} at the Department of Chemical Sciences Laboratory, University of Johannesburg, Doornfontein Campus, South Africa.Each spectrum was obtained and a total of 60 scans were conducted and averaged reflectance spectra were recorded. The spectra were baseline corrected, transformed using Optics Users Software (OPUS) following international standard described by Shepherd (2010). Prior to calibration, raw soil spectral data were subjected to preprocessing techniques to remove or minimize noise, enhance their signal, and select characteristic spectral features to improve the subsequent calibration models (Nawar et al., 2015). These techniques are mathematical procedures that transform reflectance measurements and are able to remove variability from light scattering effects and enhance spectral features. However, selecting the proper preprocessing technique is a herculean task attested by several works. Jananee et al. (2019) applied seven of the most common preprocessing techniques such as Savitzky-Golay (SG) first derivative, normalization by range, standard normal variate (SNV), multiplicative scatter-correction, continuum removal (CR), transformation to absorbance and application of a Savitzky-Golay first derivative with a first-order polynomial and a window size of 5nm and compared their performances within a range of multivariate calibration algorithms, and found CR to be the most appropriate technique for soil organic carbon prediction. In this study, however, baseline correction and normalization using the extended multiplicative signal correction method (EMSC) described by Kohler et al. (2005) was employed to remove outliers, minimize noise and enhance the signatures.

The mineral abundances in the soil were measured by isolating spectra in the ranges between 400 – 1200cm^{-1}, 1200 – 1800cm^{-1} and 2800 – 4000cm^{-1} in order to enhance the diagnosis of absorption features of each mineral. For the phyllosilicate minerals (kaolinite, illite, smectite), and non-phyllosilicate minerals (quartz, hematite, microcline), organic carbon, carbonate and water, the diagnostics feature occurrences. The relative abundance at selected diagnostic absorptions for each mineral was calculated in eight ranges from 425 - 500, 530 - 715, 770 - 920, 1000 - 1415, 1630 - 1700, 2830 - 2935, 3220 - 3430, 3620 – 3700cm^{-1}. This selection of optimum set of features instead of full spectrum which has been documented by many studies (Xing and Chen, 2013) attempts to remove non-informative variables to increase the predictive ability and reduce the complexity of a calibration model.

Multivariate Calibrations and Prediction Models

Spectral data analysis was performed with the commonly used multivariate statistical method - partial least square (PLS) regressions described by Yitagesu (2009). PLS regression is easily interpretable and has low computing time. It is similar to principal component (PCA) regression, as both employ statistical rotations to overcome the problem of high dimensionality and multicollinearity. Firstly, principal component analysis (PCA) was carried out on spectral data which showed that the first two components accounted for 84% of the total variance. Partial least square regression (PLSR) was used to fit sample spectra with soil properties such as soil texture, soil consistency, and compaction variables. This technique is a widely used multivariate tool in quantitative spectroscopy and proven to be very effective due to its ability to handle multi-collinearity (Wold et al., 2001).

The ability of the PLSR method to predict different soil properties were evaluated based on statistical indices such as coefficients of determination (R^2, Equation (1)), root mean square errors (RMSE, Equation (2)), and relative performance difference (RPD, Equation (3)) between MIR spectra and conventional soil properties.

The former measures the proportion of the total variance accounted for by the model, while the latter is the standard deviation of the difference between the measured and the predicted values. A good prediction is assumed to have small standard error and large R^2 and ratio of performance to deviation (RPD). Chang et al. (2001) proposed that for predictions of soil properties using infrared spectroscopy, RPD values below 1.4 have no predictive ability, those with RPD between 1.4 and 2.0 are acceptable and improvable, and those with RPD values above 2.0 have excellent predictive ability.

$$R^2 = 1 - \frac{SS_{error}}{SS_{total}} \quad \text{.....(1)}$$

$$RMSE = \sqrt{\frac{1}{n}\sum_{i=0}^{n}(y_i - y_p)^2} \quad \text{.....(2)}$$

$$RPD = \frac{SD}{RMSE} \quad \text{.....(3)}$$

n - total number of observations;
y_i - observed value;
y_p - estimated value;
SS_{error} - sum of squared errors between estimated and observed values;
SS_{total} - sum of squared deviations of each response variable from its mean;
SD - standard deviation

Results and Discussions

Geotechnical properties of soils

Descriptive statistics of geotechnical properties of the 50 soil samples are summarized in Table 1 with detailed percentages of sand (≥ 0.075mm), silt (0.002mm) and clays (0.001mm) of high variability. Sand ranges from 44 – 81% across the three lithologies. High percentage of fines (silt and clay) occurs in migmatite gneiss (MGR) (10 – 68%) and meta-sediment (MSVR) (11.2 – 71%) units than the old granite (OGR) (11.8 – 31%) unit. This result indicates the influence of high weathering of the parent rock.

The result of liquid limit and plasticity index of the soil samples are plotted on the Casagrande plasticity chart (Fig. 3), which indicates that the tested soils lie mostly above the A-line and are classified as inorganic clayey silty sand (SC, SM, SC-SM) soils of low – moderately high plasticity under the Unified Soil Classification System (USCS). The soils have moderately high liquid

Table 1: Summary of geotechnical properties of 50 representative soil samples

	Sand %	Silt %	Clay %	LL %	PL %	PI %	OMC %	MDD mg/m^3	CBRu %	CBRs %
	Migmatite-Gneiss region (MGR)									
Mean	65.3	20.9	30.5	30.3	16.4	13.9	14.2	1.71	7.15	3.12
Std. Dev.	9.61	9.49	13.7	9.11	7.50	4.57	4.05	0.27	5.14	1.64
Minimum	51.0	10.2	10.0	17.4	4.7	3.8	8.12	0.89	2.1	1.09
Maximum	85.0	50.8	68.0	53.0	36.9	24.4	25.0	2.61	30.4	10.6
Soil class	SC,	SM,	SC-SM,	SP-SM						
	Older Granite region (OGR)									
Mean	54.7	17.4	24.7	24.5	14.9	9.62	13.5	1.72	18.5	9.46
Std. Dev.	9.22	5.15	5.96	6.07	3.76	4.11	2.94	0.13	6.82	2.01
Minimum	44.0	11.8	14.0	16.5	8.6	4.6	8.9	1.58	10.4	7.5
Maximum	67.0	24.2	31.0	32.4	19.0	15.3	17.0	1.91	28.4	12.3
Soil class	SC,	SC-SM,	GC-GM							
	Meta-sediment/meta-volcanic region (MSVR)									
Mean	62.1	22.3	35.7	36.9	20.6	15.5	15.7	1.60	7.83	3.06
Std. Dev.	9.15	9.09	15.9	6.29	5.29	4.74	3.30	0.14	3.98	1.19
Minimum	51.0	11.2	15.0	26.5	10.4	9.3	10.1	1.4	3.0	1.26
Maximum	81.0	44.3	71.0	46.5	30.7	22.6	21.1	1.86	14.7	5.54
Soil class	SC,	SM,	SC-SM,	MH						

Note: Liquid limit (LL), plastic limit (PL), plasticity index (PI), optimum moisture content (OMC), maximum dry density (MDD), soaked and unsoaked California Bearing Ratio (CBRs, CBRu), silty sand (SM), clayey sand (SC), silty clay mixture (SC-SM), poorly graded silty sand mixture (SP-SM), silt of high plasticity (MH) and gravelly silty clay mixture (GC-GM).

limit which varies from 16.5 to 53%, which is influenced by the high content of clay (10 – 68%) particularly at MGR and MSVR regions. Since liquid and plastic limits are dependent on the type and amount of clay in the soil, they are useful parameters in the recognition of the clay fraction in the soil.

The optimum moisture content (OMC) increased with decreasing maximum dry density (MDD) from 8.1 - 25.0% and 0.9 – 2.6mg/m^3 respectively with highest occurrence (25.0%) in the MGR. The CBR quantitatively evaluates the inherent strength of soils in order to design a road pavement for a particular strength of subgrade. It is a point load test that can be carried out on almost all kinds of soils ranging from clay to gravel (Garg, 2009). The result presented in Table 1 shows a partially low soaked CBR values ranging between 1.09 – 12.3%. This confirms that very poor clayey lateritic soils were used for the subgrade and sub-base course on the pavement.

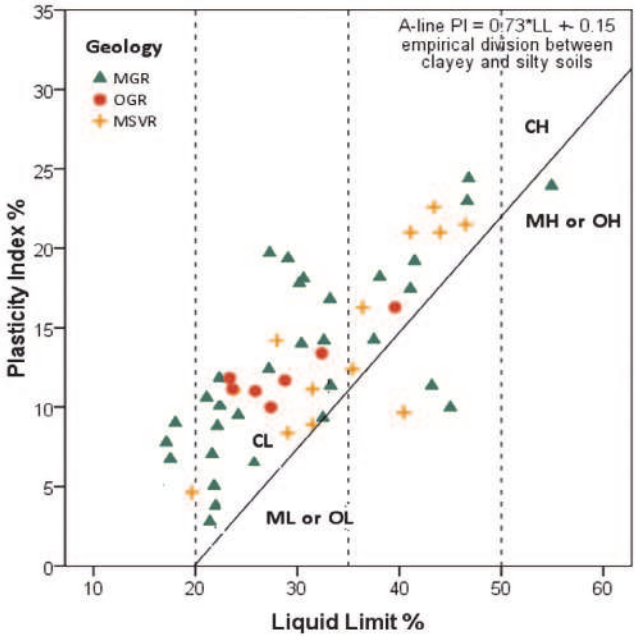

Fig. 3: Scatterplot of soil samples showing the degree of plasticity

Spectra Characteristics of different soils

The soil spectra presented (Fig. 4) show typical absorption features that are assigned based on the work of Kasprzhitskii et al. (2018), Petit and Madejova (2013), Yavna et al. (2015) and Janik et al. (2009). Strong diagnostics occur around region 500, 1000, 3000 and 3600 cm^{-1} with several stretching and bending bands that are attributed to mineral and organic components in soil.

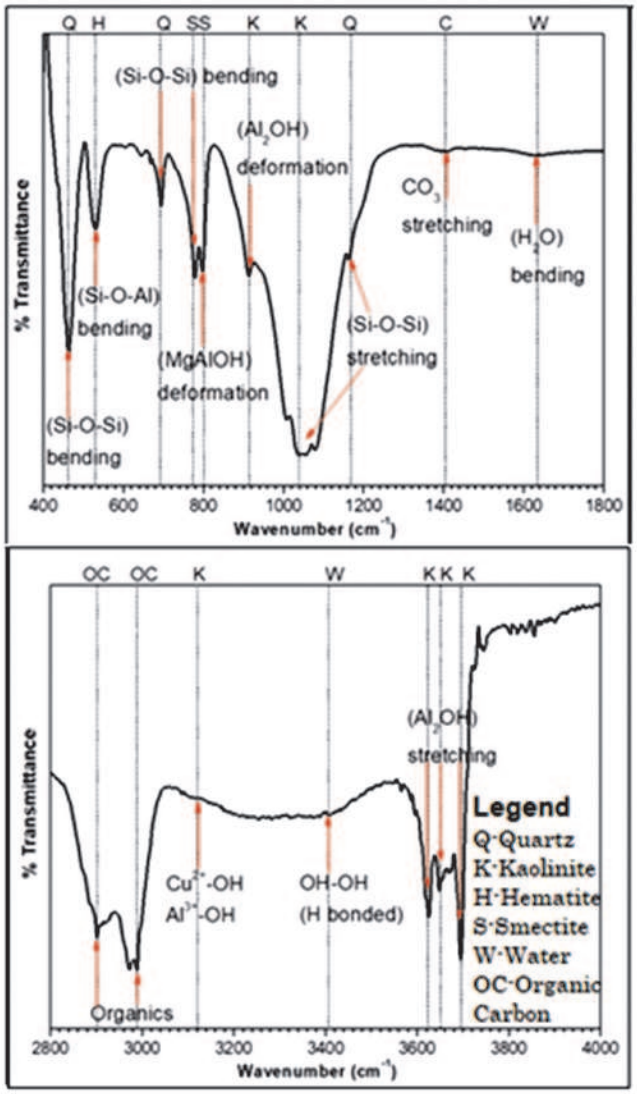

Fig. 4: A typical reflectance spectrum of a soil material.

The presence of hydroxyl (-OH) stretching and bending occurs at the 3750 – 3300 cm^{-1} and 950 – 850 cm^{-1} regions, while the Si-O stretching modes occur at the 1150 – 950 cm^{-1}and 550 – 400 cm^{-1} regions corresponding to vibrations of Si-O-Al and Si-O-Si such as kaolinite and smectite groups (Stenberg, 2010). The low reflectance around 3600cm^{-1} attests to high mineral absorption of clay minerals and additional distinct absorption bands at 1413 cm^{-1}, 695 cm^{-1} and 795 cm^{-1} assigned to CO^3 stretching and CO^3 deformation caused by the presence of calcite in the samples.

Performance of partial least square regression

Partial least square regression is a technique that attempts to combine principal component analysis and

multiple regressions (Wold *et al.,* 2001). The summary of the prediction models (Table 2) revealed an excellent performance by MIR (R^2 = 0.86, RMSE = 1.28%, RPD = 4.2) particularly for clay content compared to low R^2 = 0.5 reported by Waruru et al. (2014) in NIR region. This may be associated with the overtones and combination of band overlaps experienced in near infrared regions (NIR).

Table 2: Summary of statistics and prediction model performance indicators for PLSR

SOIL ATTRIBUTES	MSE	RMSE	R^2	RPD
Sand %	2.7	1.64	0.77	3.18
Clay %	1.63	1.28	0.86	4.25
LL %	2.36	1.78	0.72	2.46
PL %	2.13	1.46	0.76	3.14
PI %	0.99	1.21	0.78	3.64
CBRs %	2.05	1.75	0.72	2.51

Soriano-Disla et al. (2014) recognized the efficiency of MIR to make better predictions on soil properties. The prediction model for sand also yielded RMSE = 1.6, R^2 = 0.77 and RPD = 3.18. Similarly, liquid and plastic limits as well as plasticity index predictions resulted in RMSE (1.2 – 1.7), R^2 (0.72 – 0.78) and RPD (2.4 – 3.6). The performance of soaked CBR prediction model was equally satisfactory with RMSE = 1.75, R^2 = 0.72 and RPD = 2.5. The regression equations for the six parameters are summarized in Table 3. This result conforms to the outcomes of Yitagesu *et al* (2009), which established the capability of predicting geotechnical parameters such as cation exchange capacity (CEC) and CBR from spectra data.

Table 3: Summary of prediction model coefficients for soil properties

Coeff.	Sand	Clay	LL	PL	PI	CBRs
Inter.	63.2	27.3	30.3	19.4	10.9	16.5
PC1	0.01	-0.05	-0.07	-0.06	-0.01	0.01
PC2	-0.14	0.136	-0.03	0.134	-0.16	-0.01
PC3	-0.084	0.067	0.174	0.11	0.064	-0.08

Conclusions

Reflectance spectroscopy was employed to predict clay, sand LL, PL, PI and CBRs of soils from Ilorin – Kabba highway. The results were in line with previous studies. The results of the models showed strong correlation and high performance with soil texture, plasticity and CBR ($r > 0.7$) suggesting that the findings would theoretically allow MIR to estimate the properties.MIR absorption features confirmed the presence of phyllosilicate minerals by their diagnostic absorption peaks. Depth, width and area of absorption bands were significantly associated with plasticity and CBR (p-value < 0.01, r = 0.6), and co-variant minerals at 1200 - 490 cm^{-1} regions. Partial Least Square Regression (PLSR) model was established and showed high regression for soil texture, plasticity and CBR ($r > 0.7$). Existing performance indices indicates lower root-mean-square-error (RMSE) and higher ratio-of-performance-to-deviation (RPD) too.

References

AICHI, H., FOUAD, Y. and WALTER, C. (2009): Regional predictions of soil organic carbon content from spectral reflectance measurements. Biosystems Engineering, Vol. 104: 442 – 446.

BROWN, D.J., SHEPHERD, K.D., WALSH, M.G., MAYA, M.D. and REINSCH, T.G. (2006): Global soil characterizations with VNIR diffuse reflectance spectroscopy. Geoderma, Vol. 132: 273 - 290

BRITISH STANDARD (BS) (1990): Methods of Test for Soils for Civil Engineering Properties BS 1377. British Standard Institution: London, UK, 143p.

CHANG, C.W., LAIRD, D. A., MAUSBACH, M. J. and HURBURGH, C.R. (2001): Near - infrared reflectance spectroscopy – principal components regression analyses of soil properties. Soil Sciences Society American Journal, Vol. 65 (2): 480–490.

CONFORTI, M., CASTRIGNANO, A. and ROBUSTELLI, G. (2015): Laboratory-based vis-NIR spectroscopy and partial least square regression with spatially correlated errors for predicting spatial variation of soil organic matter content. Catena, Vol. 124: 60 – 67.

GARG, S.K. (2009): Physical and Engineering Geology. John Wiley Sons, New York.

GOETZ, A.F.H., CHABRILLAT, S. and LU, Z. (2001): Field reflectance spectrometry for detection of swelling clays at construction sites. Field Analytical Chemistry and Technology, Vol. 5 (3): 143 – 155.

IGE, O.O., FAKEYE, A.M. and OGUNSANWO, O. (2018): Geotechnical assessment of some soils along Ilorin-Lokoja highway – implication on suitability for road construction. Bulletin of the Science Association of Nigeria, Vol. 29: 149 – 162.

JANANEE, B., THANGAM, V. and RAJALAKSHMI, A. (2019): Investigation of soils by thermal and spectroscopic analysis. Chemical Engineering Communication. doi:10.1080/00986445.2019.1680370

JANIK, L.J., FORRESTER, S.T., AND RAWSON, A. (2009): The prediction of soil chemical and physical properties from mid-infrared spectroscopy and combined partial least-squares regression and neural networks (PLS-NN) analysis. Chemometric Intelligence Laboratory System, Vol. 97: 179–188.

KARIUKI, P.C., VAN DER MEER, F. and SIDERIUS, W. (2003): Classification of soil based on engineering indices and spectra data. International Journal of Remote Sensing, Vol. 24: 455 – 469.

KASPRZHITSKII, A.; LAZORENKO, G.; KHATER, A. and YAVNA, V. (2018): Mid-Infrared Spectroscopic assessment of plasticity characteristics of clay soils. Minerals, Vol. 8 (5): 1–18.

MOUSAVI, F., ABDI, E., FATEHI, P., GHALANDARZADEH, A., BAHRAMI, H.A., MAJNOUNIAN B. and ZIADI, N. (2021): Rapid determination of soil unconfined compressive strength using reflectance spectroscopy. Bulletin of Engineering Geology and the Environment, 1-16.

NIGERIAN GEOLOGICAL SURVEYS AGENCY (NGSA) (2004): Geological map of Nigeria. 1:2000000, NGSA, Abuja, Nigeria.

PETIT, S. and MADEJOVÁ, J. (2013): Fourier Transform Infrared Spectroscopy. In Handbook of Clay Science, Bergaya, F., Lagaly, G., (eds.): Elsevier, Amsterdam, The Netherlands, Vol. 5: 213–231. ISBN 9780080993713.

ROSSEL, R.A.V. and BEHRENS, T. (2010): Using data mining to model and interpret soil diffuse reflectance spectra. Geoderma, Vol. 158: 46 – 54.

SHEPHERD, K. D. (2010): Soil spectral diagnostics infrared, X-ray and laser diffraction spectroscopy for rapid soil characterization in the Africa Soil Information Service. In 19th World Congress of Soil Science, Soil Solutions for a Changing World, 1 - 6 August 2010, Brisbane, Australia.

NAWAR, S., BUDDENBAUM, H. and HILL, J. (2015): Estimation of soil salinity using three quantitative methods based on visible and near infrared reflectance spectroscopy: a case study from Egypt. Arabian Journal of Geosciences, Vol. 8: 5127 – 5140.

SORENSEN, L.K. and DALSGAARD, S. (2005): Determination of clay and other soil properties by near infrared spectroscopy. Soil Science Society of America Journal, Vol. 69: 159-167.

SORIANO-DISLA, J.M., JANIK, L.J., VISCARRA ROSSEL, R.A., MACDONALD, L.M. and MCLAUGHLIN, M.J., (2014): The performance of visible, near-, and mid-infrared reflectance spectroscopy for prediction of soil physical, chemical, and biological properties. Applied Spectroscopy Review, Vol. 49: 139 – 186.

SRIDHARAN, A. (2014): Soil clay mineralogy and physico-chemical mechanisms governing the fine-grained soil behaviour. Indian Geotechnical Journal, Vol. 44: 371 – 399.

STENBERG, B., VISCARRA ROSSEL, R.A., MOUNEM MOUAZEN, A. and WETTERLIND, J. (2010). Visible and Near Infrared Spectroscopy in Soil Science. Advance Agronomy, Vol. 107, 163–215.

TIAN, Y., ZHANG, J., YAO, X., CAO, W. and ZHU, Y. (2013): Laboratory assessment of three quantitative methods for estimating the organic matter content of soils in China based on visible/near-infrared reflectance spectra. Geoderma, Vol. 202–203, 161–170.

WARURU, B.K., SHEPHERD, K.D., NDEGWA, G.M., KAMONI, P.T. and SILA, A.M. (2014): Rapid estimation of soil engineering properties using diffuse reflectance near infrared spectroscopy. Biosystems Engineering, Vol. 121, 177-185.

WOLD, S., SJOSTROM, M. and ERIKSSON, L. (2001): PLS–Regression: A basic tool of Chemometrics. Chemometric Intelligence Laboratory System, Vol. 58, 109.

XING, L. and CHEN, L (2013): Quantitative analysis of near infrared spectroscopy by combined stationary wavelet transform support vector machine. Spectroscopy Letters, Vol. 46: 47-53

YITAGESU, F.A., VAN DER MEER, F., VAN DER WERFF, H. and ZIGTERMAN, W. (2009): Quantifying engineering parameters of expansive soils from their reflectance spectra.Engineering Geology, Vol. 105 (3/4), 151-160.

YAVNA, V.A., KASPRZHITSKII, A.S., LAZORENKO, G.I. and KOCHUR, A.G. (2015): Study of IR spectra of a poly-mineral natural association of phyllosilicate minerals. Optical Spectroscopy, Vol. 118, pp. 529–536.